

Màster en Recerca en Enginyeria de Processos Químics



**Ammoniun removal from
wastewater by liquid-liquid
membrane contactors**

Author: Aurora Alcaraz Segura

Supervisor: César Valderrama

Universidad Politécnica de Catalunya

December 2012

Abstract

Removal of ammonia from wastewater generated in a waste treatment plant by a membrane contactor was studied at lab scale. The treated wastewater will be applied in the Hydrogen and Oxygen production by electrolysis via renewable energies. The aim of this study relies on fulfill the process requirements in the electrolysis, since the water used in the electrolysis process must be almost pure water due to efficiency process of Hydrogen and Oxygen production decreases with the ions in the dissolution.

The residual ammonium concentration of the aqueous stream feeding the membrane distillation step ranging between 1 to 5 ppm is not removed and arrives to the electrolysis step generating an increase in the conductivity. So the use of a liquid-liquid membrane contactor is proposed to reduce ammonium (NH_4^+) concentration before membranes distillation step.

The experimental set-up was performed by a contactor (Liqui-cel X30 HF (Celgard, USA)) which works in close and open loop mode configuration. In close circuit, it was used a tank of 10 liters to storage ammonium solution and in open circuit it was used 25 liters as initial ammonium volume. A pump (Cole Parmer instrument) was used to feed the contactor from the tank. An aqueous ammonium solution with a low concentration is in the inner side of the membrane contactor (Lumen) and sulphuric acid solution goes in the outside of the membrane contactor (Shell). The pH plays a very important role in the chemical equilibrium; for that reason is motorized during the experiments.

On the other hand, it has been carried out the simulation of a mathematical model used by various authors to validate the experimental results by COMSOL Multiphysics program.

Index

1. Index of Tables.....	5
2. Index of Figures	7
3. Notations	9
4. Introduction.....	11
4.1 Aqueous solution chemistry of the system $\text{NH}_3 - \text{NH}_4^+ - \text{H}_2\text{O}$	12
5. Membrane processes for the removal of ammonium and ammonia.....	14
5.1 Introduction.....	14
5.2 Membrane process	14
6. Membrane contactors.....	16
6.1 Hollow fiber membrane modules.....	18
6.1.1 Longitudinal flow modules	18
6.1.2 Cross-flow modules	18
6.1.3 Coiled modules.....	19
7. Applications of membranes contactors	20
8. Membrane contactors for ammonium removal.....	25
8.1 Mass transfer in membrane contactors	25
8.2 Mathematical model development for the removal of ammonium from aqueous solution using contactors.....	27
8.2.1 Close loop operation mode.....	27
8.2.2 Open loop operation mode	33
9. Objectives and Methodology	33
9.1 Objectives	33
9.2 Methodology	34
9.2.1 Reagents	34
9.2.2 Membrane contactors	34
9.2.3 Experimental procedure.....	35
9.2.4 Monitoring protocol.....	37
10. Results and discussion	39
10.1 Results and discussion for close loop operation mode	42
10.2 Results and discussion for open loop operation mode.....	47
11. Conclusions.....	56
12. Annex.....	57
12.1 Annex 1. Summary of the experimental results.....	58

12.2	Annex 2. Graphics of experimental results.....	59
12.3	Annex 3. Poster exhibited in Milan COMSOL Congress in October 2012.....	61
12.4	Annex 4. . Paper exhibited in Milan COMSOL Congress in October 2012	62
13.	References.....	71

1. Index of Tables

Table 1. Membrane process	15
Table 2 Advantages and disadvantages of membrane contactors.	17
Table 3. Specifications of the hollow fiber membrane contactor	34
Table 4. Operation conditions in the experiments	35
Table 5. Summary of the experiments at conditions evaluated	38
Table 6. Model equations and boundary conditions	39
Table 7. Initial values of parameters to be estimated	40
Table 8. Nominal values of membrane contactor parameters	41
Table 9. Experimental results and RMSD with variable pH in close loop configuration with flow rate 0.26 l/min and initial concentration of ammonium of 15 ppm.....	43
Table 10. Experimental results and RMSD with variable initial concentration in close loop configuration with flow rate 0.26 l/min and pH 10.4	44
Table 11. Experimental results and RMSD with variable flow rate in close loop configuration with initial concentration of ammonium of 15 ppm and pH 10.1.....	46
Table 12. Optimal work conditions in close loop configuration	46
Table 13. Experimental results and RMSD with variable pH in open loop configuration with flow rate 0.26 l/min and initial concentration of ammonium 5 ppm.....	48
Table 14. Experimental results and RMSD with variable flow rate in open loop configuration with initial concentration of ammonium of 5 ppm and pH 9.9.....	50
Table 15. Experimental results and RMSD with variable initial concentration of ammonium in open loop configuration.....	51
Table 16. Optimal work conditions in open loop configuration.....	51
Table 17. Experimental results and RMSD with variable initial concentration of ammonium in open loop configuration with wastewater.....	54

Table 18. Parameters estimated for close and open loop configuration model..... 54

Table 19. Characteristics parameters for close and open loop configuration model 55

2. Index of Figures

Figure 1. Pilot plant developed for Greenlysis project (CETaqua)	11
Figure 2. Equilibrium Ammonia-Ammonium dependent of pH	13
Figure 3. Membrane contactor	16
Figure 4. Longitudinal flow membrane contactor module scheme	18
Figure 5. Cross-flow membrane contactor module scheme.....	19
Figure 6. Coiled membrane contactor module scheme	20
Figure 7. Principle of pertraction	22
Figure 8. Principle of emulsion pertaction	23
Figure 9. Principle membrane gas absorption	24
Figure 10. Transport steps for separation of NH ₃ molecules through the HFMC	25
Figure 11. Principle of the extraction process	26
Figure 12. Experimental setup	27
Figure 13. Concentration profile for the species j at a particular time when it moves from lumen side towards shell side through a microporous hydrophobic membrane	32
Figure 14. a) Cross section of a membrane module showing the fibers. b) Hollow fiber with the transport phenomena. c) Membrane contactor. d) Side view of the entrance to the hollow fibers.....	35
Figure 15. Membrane contactor operated by liquid-liquid extraction (Close loop configuration)	36
Figure 16. Membrane contactor for the removal of dissolved ammonia (Open loop configuration).....	36
Figure 17. Influence of feed solution pH on the fractional removal in the close loop configuration, with flow rate 0.26 l/min and initial ammonium concentration of 15 ppm. Comparison between simulated values and experimental data.	42

Figure 18. Influence of initial ammonium concentration in fractional removal in the close loop configuration with flow rate 0.26 l/min and pH 10.4. Comparison between simulated values and experimental data. 43

Figure 19. . Influence of flow rate on the fractional removal in the close loop configuration with Initial concentration of ammonium 15 ppm and pH 10.1. Comparison between simulated values and experimental data. 45

Figure 20. Influence of feed solution pH on the variation in fractional removal in the open loop configuration with $Q = 0.26$ l/min and initial concentration of ammonium 5 ppm. Experimental values 47

Figure 21. Influence of flow rate on the variation in fractional removal in the open loop configuration with pH 9.9 and initial concentration of ammonium 5 ppm. Experimental values 48

Figure 22. Influence of flow rate on the variation in fractional removal in the open loop configuration with pH 9.9 and initial concentration of ammonium 5 ppm. Comparison between simulated values and experimental data. 49

Figure 23. Influence of initial concentration on the variation in fractional removal in the open loop configuration with pH 9.9 and $Q = 0.26$ l/min. Experimental values 50

Figure 24. Influence of initial concentration on the variation in fractional removal in the open loop configuration with wastewater with $Q = 0.26$ l/min and pH 9.8. Experimental values 52

3. Notations

b	Membrane thickness (m)
C	Concentration (mol/m ³)
d	Diameter (m)
D	Diffusivity (m ² /s)
H	Henry's constant (Pa m ³ /mol)
k	Mass transfer coefficient (m/s)
K _b	Ionization equilibrium constant of ammonia
L	Length of the module (m)
M	Molecular weight (g/mol)
N	Number of fibers
p	Partial pressure (Pa)
Q	Feed flow rate (m ³ /s)
r	Radial coordinate (m)
R	Radius of the lumen (m)
R _g	Universal gas constant (J/mol K)
R _j	Rate of generation of component j due to chemical reaction (mol/s m ³)
t	Time (s)
T	Temperature (K)
U	Velocity inside the fiber (m/s)
V	Volume of feed tank (m ³)
Z	Axial coordinate (m)

Subscript

0	Initial
a	Ammonia
am	Ammonium
air	Air
c	Combined
g	Gas
l	Inner
int	Liquid-gas interface
j	Combined ammonia and ammonium

k	Knudsen diffusion
m	Membrane
o	Outer
pore	membrane pore
tank	Tank
Z	Axial direction

Superscript

-	Average
~	Vector
g	gas

Greek letters

ϵ	Porosity of the membrane
τ	Tortuosity of the pore
B	Fractional removal ammonia

4. Introduction

This Master project has been developed inside the European project Greenlysis "Hydrogen and Oxygen production by electrolysis via renewable energies to reduce environmental footprint of a waste water treatment plant (WWTP)." The project is devoted to the use of renewable energy to produce Hydrogen and Oxygen from water, using treated wastewater as raw material. Figure 1 shows the diagram process of the pilot plant located in (Montornès del Vallès, Barcelona) with a daily capacity of 2 m³/day

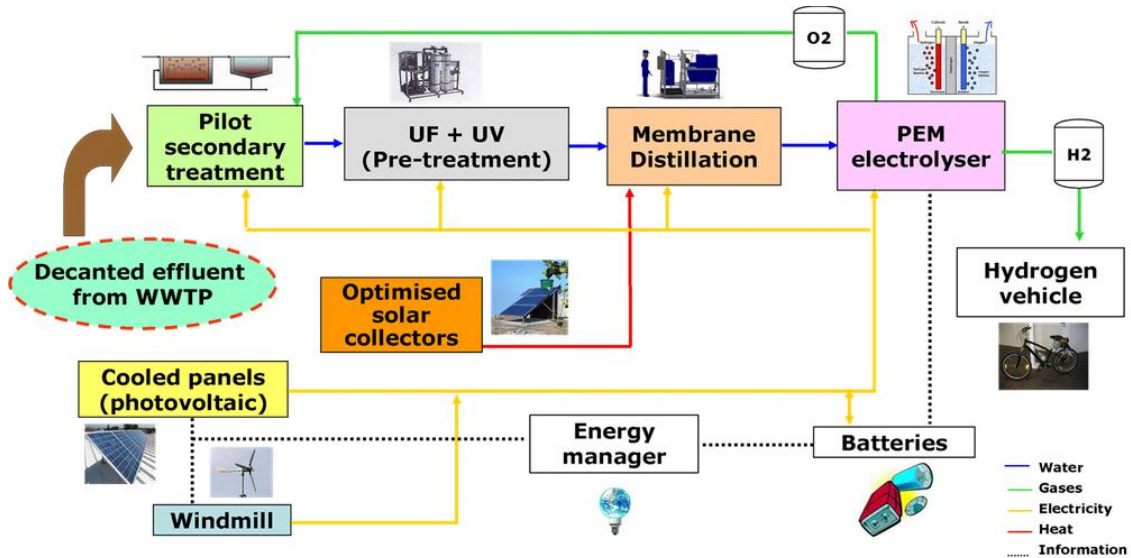


Figure 1. Pilot plant developed for Greenlysis project (CETAqua)

The effluent from the WWTP is pre-treated in batch mode with an ultrafiltration (UF) step and kept in a storage tank. Afterwards a disinfection process is applied by Ultraviolet (UV) treatment. The purification process of the pre-treated effluent is carried out through in a Membrane Distillation unit in order to obtain pure water (10-15 L/day). The next step is the Electrolysis unit with a flow-rate of 1 L/h of pure water to produce pressurized (15 bar) H₂ (0.6 Nm³/h) and O₂ (0.3 Nm³/h) to produce Hydrogen and Oxygen. The pressurized hydrogen is used to power a bike which is filled directly from the electrolyser H₂ tank. The pressurized Oxygen is used in a biological reactor to treat wastewater in order to save energy (power for air supply). The whole pilot plant energy demand will be powered by renewable photovoltaic panels and wind equipment. One third of photovoltaic panels will be refrigerated in order to decrease temperature and increase the efficiency.

The aims of the Greenlysis project are to replace the current conventional aeration system of the WWTP by O₂ obtained from Electrolysis. Additionally to reduce the fossil fuel consumption and CO₂ emissions of a vehicle (bike) by using the H₂ obtained in the same

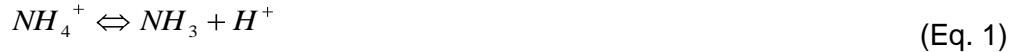
step. Additionally the pilot plant is operated by photovoltaic and wind energy which leads to a significant reduction in greenhouse gasses (GHG) emissions.

The aim of this Master project relies on a process requirement of the Greenlysis project. Thus, the conductivity of the Electrolysis input stream should be lowest than $1 \mu\text{S}\cdot\text{cm}^{-1}$. However, the residual ammonium concentration of the aqueous stream feeding the membrane distillation step ranging between 1 to 5 ppm is not remove and arrive to the Electrolysis step generating an increase in the conductivity go to values of $10\text{-}20 \mu\text{S}\cdot\text{cm}^{-1}$. It makes that efficiency of Electrolysis unit be lower. Then is necessary to remove or reduce the ammonium concentration in aqueous stream leaving the UF unit before Membranes distillation step in terms of suitable conductivity for the Electrolysis unit.

4.1 Aqueous solution chemistry of the system $\text{NH}_3 - \text{NH}_4^+ - \text{H}_2\text{O}$

Ammonia is a colorless gas with a characteristic odor, very soluble in water. Its aqueous solutions are alkaline and have a corrosive effect in front to metals and tissue (Busca and Pistarino 2003). The pH in an aqueous solution of 0.1 M is 11.2, which is characteristic of a weak base ($\text{pK}_a = 9.3$).

Ammonia in water exists in free and ionic forms under equilibrium:



The Henry's law constant and equilibrium dissociation constant for the $\text{NH}_4^+ - \text{NH}_3 - \text{water}$ system can be expressed as follows:

$$H_{\text{NH}_3} = \frac{\text{NH}_3_{aq}}{P_{\text{NH}_3}} \quad (\text{Eq.2})$$

$$k_a = \frac{[\text{NH}_3][\text{H}^+]}{[\text{NH}_4^+]} \quad (\text{Eq. 3})$$

The Henry's constant, H_{NH_3} , can be interpreted as the physical solubility parameter, which reflects the level of the free form of the gas dissolved in the water but does not represent its subsequent fate on dissolution. On the other hand, k_b is the dissociation equilibrium constant for dissolved ammonia, which represents the level of NH_4^+ ions.

Equations (2) and (3) can be rearranged to obtain an expression for NH_4^+ concentration in term Henry's law constant, dissociation constant, gas partial pressure and protons concentration, obtaining the equation 3 (Agrahari et al., 2012):

$$[\text{NH}_4^+] = \frac{[\text{H}^+][\text{NH}_3]}{k_a} = \frac{H_{\text{NH}_3} P_{\text{NH}_3} [\text{H}^+]}{k_a} \quad (\text{Eq. 4})$$

The total concentration of ammonia can be written as the sum of the molar concentrations of ionic and free form of NH_3 :

$$[\text{NH}_3]_{\text{total}} = [\text{NH}_3] + [\text{NH}_4^+] = H_{\text{NH}_3} p_{\text{NH}_3} \frac{[\text{H}^+]}{K_a} \quad (\text{Eq.5})$$

The predominant species for the ammonium equilibrium in water are shown in Figure 2. For values below the pK_a (9.3), ion ammonium is greater than ammonia. At pH 9.3 both the ionic form as the free species were found to 50% in solution. When pH value is higher than the pK_a , it is found ammonia as predominant compound.

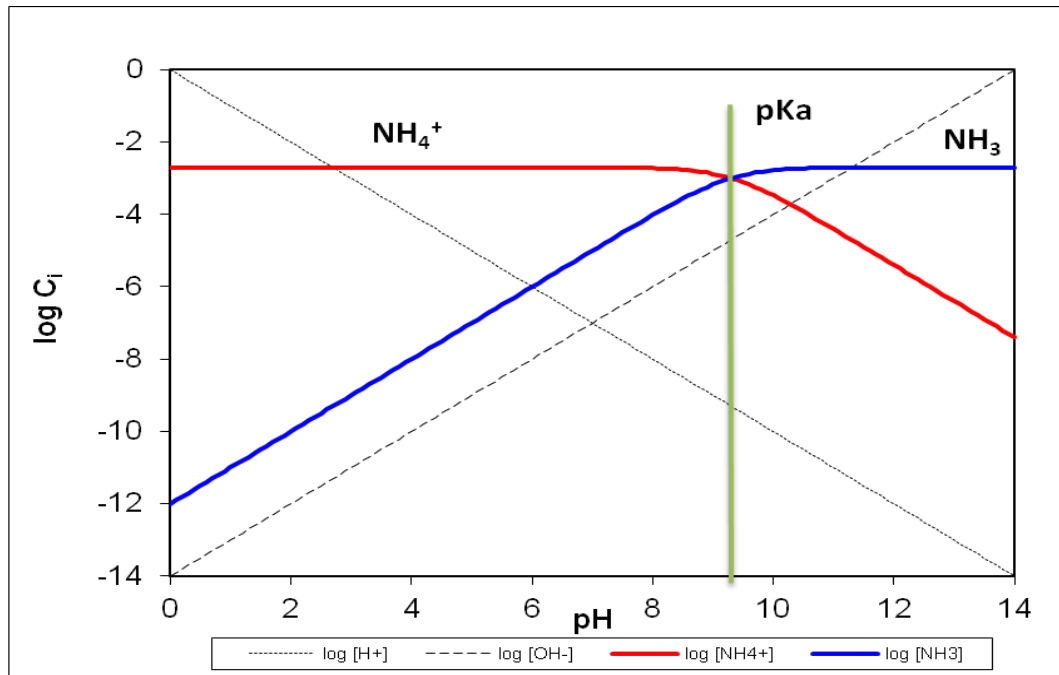


Figure 2. Equilibrium Ammonia-Ammonium dependent of pH

In consequence, many physical and chemical properties of ammonia are a function of pH. For instance, the ammonia solubility in water increases when pH decreases. The ammonia can volatilize freely from its solutions with water at high pH. The ammonia is used primarily as a nitrogen source in the generation of fertilizers; as refrigerant, in the manufacture of nitric acid and other chemical reagents such as sulfuric acid, cyanides, amides, nitrites and intermediaries dyes; as a nitrogen source in the production of synthetic fiber monomers and plastics; as corrosion inhibitor in oil refining and other industries such as paper, extractive, food, fur and pharmaceutical industries. Some of the mentioned industries generate wastewater containing dissolved toxic gases, such as ammonia, in small concentrations. For example, industries that produce urea fertilizers have dissolved ammonium (500-2000 ppm) in their wastewater (Mandowara and Bhattacharya, 2011).

Due to use of this compound to industrial, domestic and agriculture sector, ammonia is one of the major inorganic pollutants in the water. Then the removal of this substance is due to two main reasons (Jorgense and Wheatley, 2003; Moazed, 2008):

- Its extreme toxicity to marine life (concentrations below 0.01 ppm have negative effects on fish, while 0.1 ppm can be lethal to other species) (Mandowara and Bhattacharya, 2011).
- It can be bio-oxidized by nitrifying organisms to nitrites and nitrates.

This project also takes into account a third reason for removal. As has been mentioned above, the ammonia impact in higher conductivity which is not desired for electrolysis step in the hydrolysis process for producing hydrogen and oxygen, which makes necessary to remove this compound.

5. Membrane processes for the removal of ammonium and ammonia

5.1 Introduction

Several techniques are available for the removal of dissolved ammonia, such as air stripping, break-point chlorination, selective ion exchange, biological nitrification and denitrification and adsorption (Sarioglu, 2005). Removal by conventional extraction or stripping processes may not be suitable for low-concentration wastewater. Break-point chlorination suffers from several disadvantages including large treatment volume, associated risk, difficulty of pH control, and high chemical costs. The ion-exchange process requires expensive organic resins and large quantities of eluent solution (Sarioglu, 2005). Biological nitrification and denitrification are slow processes and require large treatment vessels. Therefore, most of the available treatment processes are not particularly effective at low concentrations. Some of the advances made in membrane processes in last two decades allow considering this technique as potential attractive for ammonia removal.

5.2 Membrane process

Commercially, membrane filtration has a great acceptance as an important step in many of the process in several industries, as well as in water purification (Scott, 1998). Very specific separations have been obtained at ambient temperature with no phase change which makes membrane filtration a cost-effective separation method compared to others such as vacuum

filtration, and spray drying. The hydrostatic pressure is most often the driving force, but can also be electrical potential, concentration gradient, or temperature.

The processes collected in Table 1 represent the majority of commercial membrane separation technologies that could be used for $\text{NH}_3 / \text{NH}_4^+$ removal:

<i>Process</i>	<i>Type of membrane</i>	<i>Material passed</i>	<i>Material retained</i>	<i>Driving force</i>	<i>Status – typical application</i>
Reverse osmosis	Dense solution-diffusion	Water	Dissolved salts	Pressure difference 100–1000 psi	Developed (~US\$200 million per year). Drinking water from sea, brackish or groundwater; production of ultrapure water for electronics and pharmaceutical industries
Electrodialysis	Electrically charged films	Water	Ions	Voltage difference 1–2 V	Developed (~US\$200 million per year). Drinking water from brackish water; some industrial applications too
Dialysis	Finely microporous 10–100 nm	Dissolved salts, dissolved gases	Blood	Concentration differences	Developed (~US\$1.3 billion per year for artificial kidney; US\$500 million per year for artificial lung)
Gas separation	Dense, solution-diffusion	Permeable gases and vapours	Impermeable gases and vapors	Pressure difference 100–1000 psi	Developing (~US\$150 million per year). Nitrogen from air, hydrogen from petrochemical/refinery vents, carbon dioxide from natural gas, propylene and VOCs from petrochemical vents
Pervaporation	Dense, solution-diffusion	Permeable micro-solutes and solvents	Impermeable micro-solutes and solvents	Vapour pressure 1–10 psi	Developing (~US\$10 million per year). Dehydration of solvents (especially ethanol)

Table 1. Membrane process (Baker, 2000)

However, a number of processes are still in the laboratory or early commercial stage and may yet become important. One of these processes are membrane contactors. In the membrane separation processes the membrane acts as a selective barrier allowing relatively free passage of one component while retaining another. In membrane contactors the membrane function is to provide an interface between two phases but not to control the rate of passage of permeates across the membrane (Baker, 2000). Due to many advantages offered by these devices, contactors are considered as a potential technology for ammonia removal from water.

6. Membrane contactors

Hollow fiber membrane contactors (HFMC) have been used to remove volatile compounds from water and wastewater. The hollow fibers used are commonly microporous and hydrophobic (Lee et al., 2003). In this process, the feed and stripping solution are flowing on either side of a membrane. Membrane contactors are divided in two parts: an internal side (Lumen) and an external side (Shell). Since the membrane is hydrophobic, it prevents aqueous solution, which has higher surface tension, to penetrate the gas-filled pores. The volatile compounds will volatilize from the feed, diffuse through the gas-filled membrane pores, and react with the stripping solution (Zhu et al., 2005). In Figure 3 is shown a typical configuration of membrane contactor:

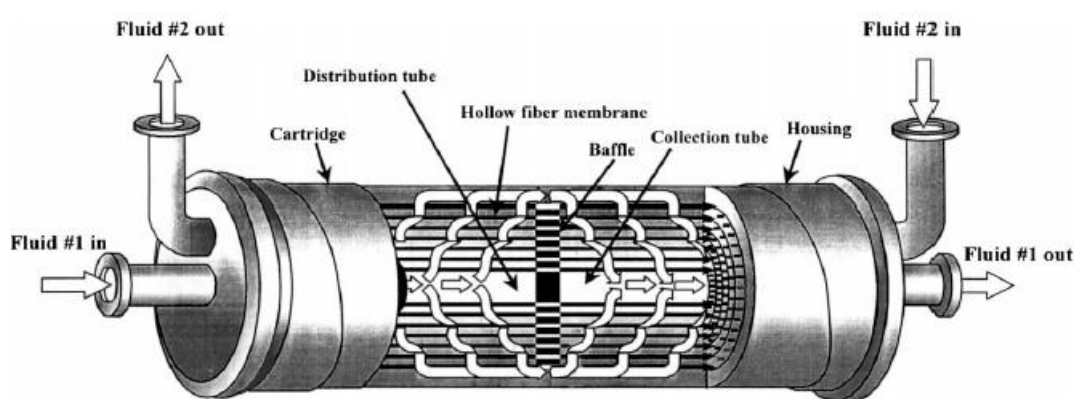


Figure 3. Membrane contactor (Gabelman, and Hwangb, 1999)

Several theoretical studies have been carried out to understand the mechanism of gas removal using a hollow fiber membrane contactor and a variety of mathematical models have been developed. The focus of most of the studies has been on ammonia (NH_3) and carbon dioxide (CO_2), which are the common impurities present in industrial wastewater effluents and gas emissions respectively (Agrahari et al., 2012).

Different types of membrane such as symmetric hydrophobic porous membranes or asymmetric membranes with ultra-thin layers can be used as a gas-liquid membrane contactor (Atchariyawut, et al., 2006; Albrecht et al., 2005). In both cases the membrane must be able to separate the contacting fluids. Typical membranes used are prepared from hydrophobic polymer materials with a high porosity.

Among various hydrophobic polymers as polypropylene (PP), polyethylene(PE), polytetrafluoroethylene (PTFE) and Polyvinylidene fluoride (PVDF), which are the most popular membrane materials (Mansourizadeh and Ismael, 2009). PVDF membranes have

excellent chemical and thermal resistance which makes them suitable for most of the corrosive chemicals and organic compounds such as acids, alkaline, oxidant and halogens. The main advantages and disadvantages of hollow fibers contactors are summarized on Table 2.

Advantages	Disadvantages
The available surface area remains undisturbed at high and low flow rates because the two fluid flows are independent. This is useful in applications where the required solvent/feed ratio is very high or very low. In contrast, columns are subject to flooding at high flow rates and unloading at lowness.	The membrane introduces another resistance to mass transfer not found in conventional operations: the resistance of the membrane itself. However, this resistance is not always important, and steps can be taken to minimize it.
Emulsion formation does not occur, again because there is no fluid/fluid dispersion.	Membranes are subject to fouling
These devices can accommodate fluids of identical density and can be operated in any orientation.	Membranes have a finite life, so that the cost of periodic membrane replacement needs to be considered.
Scale-up is more easy	The potting adhesive (e.g., epoxy) used to secure the fiber bundle to the tube sheet may be vulnerable to attack by organic solvents.
Aseptic operation is possible, a feature which can be advantageous in processes such as fermentation	The achievable number of equilibrium stages is limited by pressure drop constraints.
Be used to increase conversion with equilibrium-limited chemical reactions in general	
Interfacial area is known and is constant, which allows performance to be predicted more easily than with conventional dispersed phase contactors	
Higher efficiency is achieved with membrane contactors	
Unlike mechanically agitated dispersed phase columns, membrane contactors have no moving parts.	

Table 2 Advantages and disadvantages of membrane contactors. (Baker, 2000)

6.1 Hollow fiber membrane modules

6.1.1 Longitudinal flow modules

In these modules, the gas and liquid phases flow in parallel to each other on the opposite side of the fibers (Figure 4). The flows can be co-current or counter-current. Most of the researches on the membrane gas absorption in laboratory scale have conducted on this kind of membrane module (Kim and Yang, 2000; Lee et al, 2001; Dindore et al., 2004; Yang and Cussler, 1986) studied and discussed the construction of the parallel and cross-flow modules. They reported the results of experiments made with these modules, and described the mechanism responsible for controlling the mass transfer in the various cases. Finally, they discussed the correlations that can be inferred from their experiments, and compare these with correlations previously reported for analogous heat and mass transfer problems. Their discussion provides a basis for designing hollow fiber membrane modules for contacting both gases and liquids in other situations.

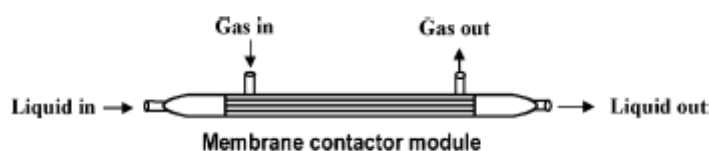


Figure 4. Longitudinal flow membrane contactor module scheme

The simplicity in manufacturing, well known fluid dynamics in shell and tube side and easiness of mass transfer estimation are the advantages of this module, while the main disadvantages is the moderate efficiency in mass transfer compared with the cross-flow module (Mansourizadeh and Ismael, 2009).

6.1.2 Cross-flow modules

In general, cross-flow operation of hollow fiber membrane contactors is preferred as it offers several advantages such as higher mass transfer coefficients, minimized shell side channeling and lower shell side pressure drop as compared to the parallel flow contactors. Physical gas absorption in a rectangular cross-flow hollow fiber gas–liquid membrane contactor has been discussed in detail by Dindore and Versteeg (2005). The performance of different parallel and cross-flow gas–liquid membrane contactors based on the equal flow per membrane area and equal flow per module volume and found that in both cases cross-flow membrane modules were more effective as compared to parallel flow modules. Details of the configuration of both types of modules are described in Figure 5.

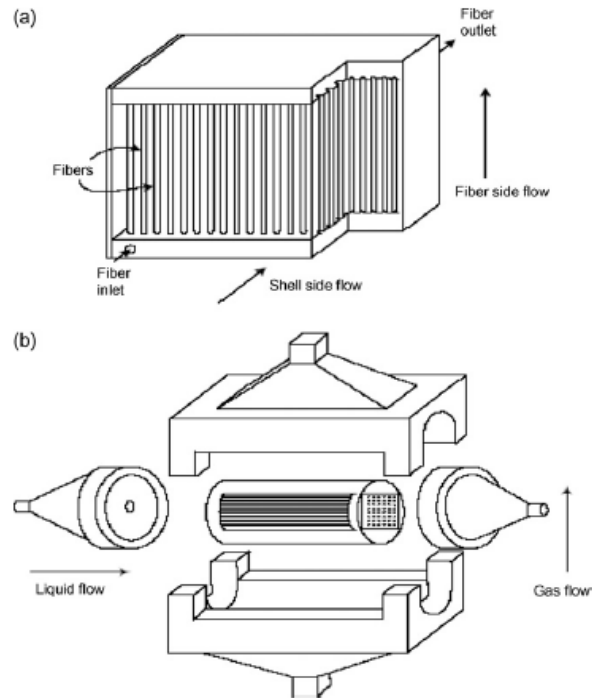


Figure 5. Cross-flow membrane contactor module scheme (Dindore and Versteeg, 2005)

6.1.3 Coiled modules

Recently, more attention is paid to the coiled modules for the ultrafiltration and nanofiltration membrane applications (Manno et al., 1998; Ghogomu et al., 2001; Mallubhotla et al., 1999). In this module curved channels are used to create secondary flow in fluid, so that the involved flow and transfer process are intensified. One important advantage of coiled module over others is its capability of simultaneous improvement on mass transfer in both lumen and shell side. Liu et al. (2005) prepared coiled hollow fiber membrane modules and examined their mass transfer performances for stripping dissolved oxygen from water. It was found that, compared with the conventional module, the mass transfer in both lumen and shell side of the coiled hollow fiber module could be remarkably enhanced. The improvements in mass transfer can be attributed to the created secondary flows (known as Dean Vortices) inside coiled fiber and the promoted turbulence on the shell. However, the number of studies on this area is rare. Figure 6 describes a coiled membrane contactor module.

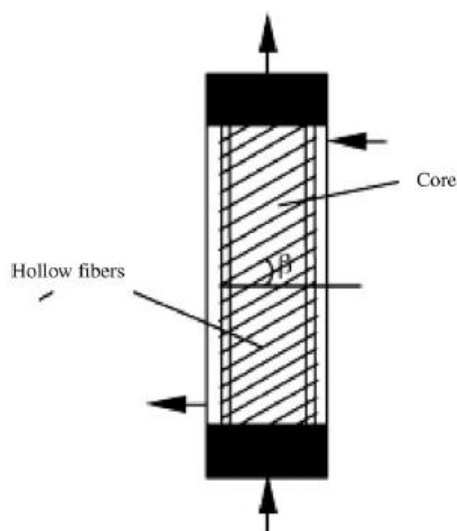


Figure 6. Coiled membrane contactor module scheme (Liu et al, 2005)

7. Applications of membranes contactors

Several researchers have carried out simulation studies of the degasification of water via convective diffusion using membrane contactors (Mandowara and Bhattacharya, 2009; Kieffer et al., 2008; Al-Marzouqi et al., 2008; Lee et al., 2001). Mandowara and Bhattacharya (2009) simulated ammonia removal by a vacuum application on the shell side and obtained concentration profiles. Kieffer et al. (2008) used computational fluid dynamics to numerically study mass transfer in a liquid-liquid-phase membrane contactor, and they observed a clear separation between the reaction and mixing zones. Al-Marzouqi et al. (2008) modeled the chemical absorption of CO_2 in Monoethanolamine (MEA) solvent using PP membrane contactors; they considered both radial and axial diffusion under the condition of complete wetting. Lee et al. (2001) studied the removal of CO_2 in a hollow fiber membrane contactor using aqueous potassium carbonate; they derived and numerically solved coupled nonlinear partial differential equations and also reported the optimal absorbent flow rate. Keshavarz et al. (2008) developed a mathematical model for membrane contactors operated under non-wet or partially wetted conditions during the simultaneous absorption of carbon dioxide and hydrogen sulphide in diethanolamine (DEA) solution. Bottino et al. (2008) experimentally and numerically studied CO_2 removal from a gas stream using aqueous monoethanolamine as an extract phase. Different commercial polypropylene capillary membranes in a membrane contactor and found the CO_2 removal efficiency were used. The experimental results were in good agreement with the predicted results. Malek et al. (1996) evaluated and studied microporous hollow-fiber membrane modules operated under partially wetted conditions. The nonlinear partial differential equations were solved using an orthogonal collocation method. The experimental results found were in good agreement with the modeling results.

McDermott et al. (2007) studied the vacuum-assisted removal of volatile and semi-volatile organic contaminants from water using hollow-fiber-based membrane contactors. They used a hybrid numerical-analytical approach and investigated the main factors controlling the removal characteristics, e.g., the Henry's law coefficient, gas-side diffusion resistance, and aqueous diffusion limitation.

Although it is difficult to introduce new technologies in industry there is still a large demand for new improved processes, especially in the field of separation technology. Stringent demands are put onto these new separation technologies in order to compete with the existing proven technologies and in order to meet stricter product quality requirements, environmental legislation, energy efficiency demands and last but not least needs for cost reduction (Klaassen et al., 2005). In order to meet these ever increasing needs there is a tendency to combine processes to a hybrid process. In a membrane contactor membrane separation is not only combined with an phase contacting process like extraction or absorption but both processes are fully integrated and incorporated into one piece of equipment. In this way advantages of both processes can be fully exploited (Klaassen et al, 2005). The membrane offers a flexible modular efficient device with a low volume and weight so that it can be easily integrated in existing installations. The extraction or absorption process can offer a very high selectivity and a high driving force for transport even at very low concentrations. Applications of membrane contactors are of interest for the chemical, petrochemical, pharmaceutical and galvanic industry for both water and gas treatment as end of pipe technology but also for product recovery and as integrated process solution (Klaassen et al., 2008).

The industrial reference installations, in the field of pertraction, emulsion pertraction and membrane gas absorption, help to gain confidence of end users in the membrane contactor technology.

- Pertraction technology

Pertraction is a non-dispersive membrane based liquid–liquid extraction process. Nonpolar organic substances such as aromatics or chlorinated hydrocarbons can be recovered from process or wastewater flows by pertraction. The organic components are removed from the water by extraction into an organic extractant, which is immiscible with water. The extractant is flowing at one side of the membrane and the water phase at the other side. The role of the membrane is to keep the phases separated and to provide a suitable interface between the two phases. The membrane itself has no selectivity. The process selectivity must come from the extractant. The interface between wastewater and extractant is immobilized using a hydrophobic microporous hollow fiber membrane by means of a small trans-membrane pressure gradient (0.1 bar) (Kiani et al., 1984; Klassen et al., 1994b, Klaassen, 1998), as can be seen in Figure 7. Contrary to conventional extraction processes there is no direct mixing of extractant in the wastewater stream.

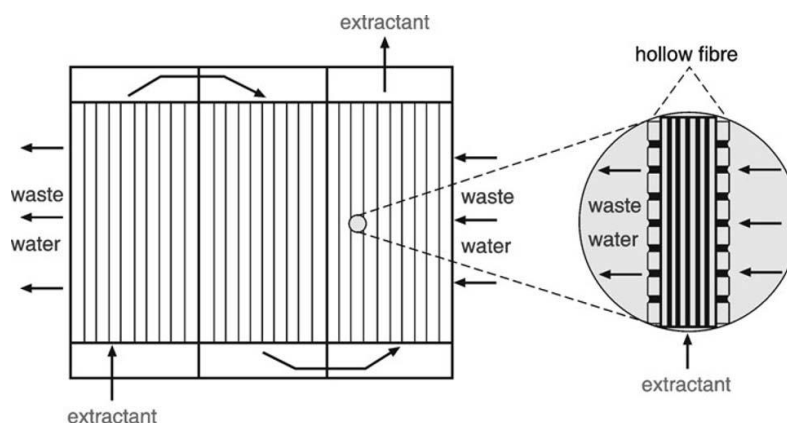


Figure 7. Principle of pertraction

Pertraction is especially suitable for removal of hydrophobic organic compounds like aromatic and aliphatic organics, chlorinated solvents (e.g., carbon tetrachloride, chloroform, tetrachloroethene and trichloroethene), PCB's, di- and tri-chlorobenzene, pesticides and higher polycyclic hydrocarbons (Klaassen et al, 2005).

Water streams containing these hydrocarbons can be found at many places:

- Effluents/process streams from pharmaceutical, off shore, automotive, paint, petrochemical and chemical-plants.
- Water originating from tank cleaning and tank storage.
- Effluents from garages dry cleaning and wood preservation.
- Contaminated ground water.
- Landfill leachate from sites containing chemical wastes.

- Emulsion pertraction technology

Emulsion pertraction is a combined extraction and regeneration process suitable for selective removal of heavy metals like copper, zinc, iron, chromium, cadmium or lead from aqueous solutions. The heavy metals can be recovered in a concentrated solution. Lifetime extension of bath liquids is an industrial application for emulsion pertraction. The principle of emulsion pertraction is also used by Commodore Separation Technologies for the recovery of Cr(VI) from waste water (Ho and Poddar, 2001). Water phase is kept apart from the emulsion phase by a hydrophobic microporous membrane. Emulsion pertraction is a process evolved from a combination of permeation through membranes and solvent extraction. (Klaassen et al., 1996). The emulsion phase consists of an organic solvent with a dissolved extractant as continuous phase with aqueous droplets of strip liquid dispersed in it. In Figure 8 it can see the principle of emulsion pertraction. The metal to be removed from the water phase is bound by the extractant present in the pores of the membrane. At the other side of the membrane the strip liquid continuously regenerates the extractant. In this way an optimal driving force for transport is maintained in the membrane contactor. The strip liquid is dispersed in the organic phase. There is no need to make this dispersion very suitable because the hydrophobic nature of the membrane keeps the waste water and aqueous strip liquid always separated.

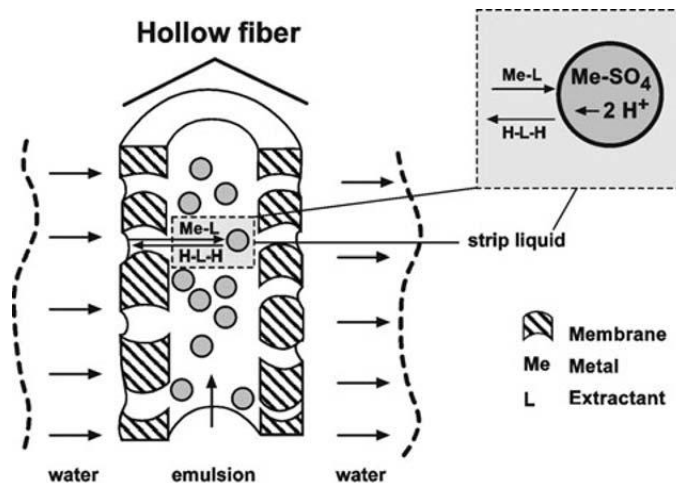


Figure 8. Principle of emulsion pertraction

- Membrane gas absorption technology

Membrane gas absorption is a gas-liquid contacting operation (Zhang and Cussler, 1985; Klaassen et al., 1996; Feron et al., 1997). The essential element in the membrane gas absorption process is a microporous hydrophobic hollow fiber membrane. The gas stream is fed along one side of the membrane at the same time an absorption solution is flowing at the other side of the membrane. The absorption liquid is chosen in such a way that it has a high affinity for components that must be removed from the gas stream. These components will diffuse through the gas filled pores of the membrane to the other side of the membrane where they are absorbed in a liquid phase. Absorption in the liquid phase takes place either by physical absorption or by a chemical reaction. This determines the selectivity of the process. The membrane used gives no contribution to the selectivity: the membrane's role is to keep the two phases separated and to provide a large contacting surface area. The process is illustrated in Figure 9 (Klaassen et al, 2005).

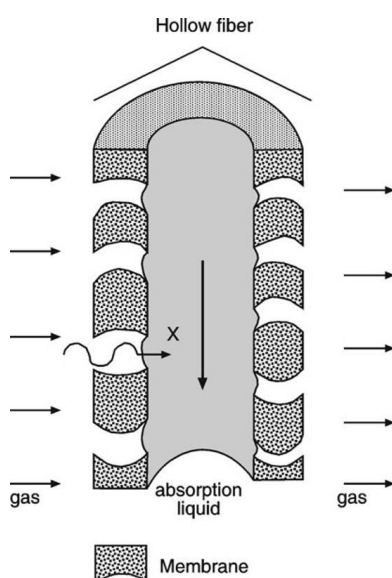


Figure 9. Principle membrane gas absorption

Membrane gas absorption can be applied for removal of those components from a gas stream where a suitable absorption liquid is available. An absorption liquid has a high affinity for the components to be removed and does not wet the membrane. The majority of absorbents used in conventional gas absorption processes can also be used for membrane gas absorption. Applications (Klaassen et al., 1996, Feron et al., 1997, Klaassen and Jansen, 2001) for the use of membrane gas absorption are listed below:

- Flue-gas and off-gas containing e.g., SO_2 , HCl , NH_3 or H_2S can be treated to meet emission standards in many industrial situations.
- Recovery and re-use of CO_2 from flue gas, biogas and off-gases in horticultural industry, beverage production and other industrial applications.
- Upgrading and desulphurization of biogas from anaerobic digesters and landfills.
- Acid gas removal and dehydration of natural gas.
- Acid gas removal from fuel gas mixtures.
- Mercury removal from natural gas, flue gas or glycol overheads.
- Olefin-paraffin separation in petrochemical industry.
- Indoor air treatment for e.g., tobacco smoke components.

8. Membrane contactors for ammonium removal

8.1 Mass transfer in membrane contactors

As described in section 1.1, in aqueous solution, ammonia exists as both protonated and non-protonated ammonia. When the aqueous solution crosses the membrane contactor, the transport of ammonia is governed by three steps (Mandowara and Bhattacharya, 2011):

- Axial diffusion
- Radial diffusion
- Convection in the lumen side

Figure 10, describes schematically the described steps:

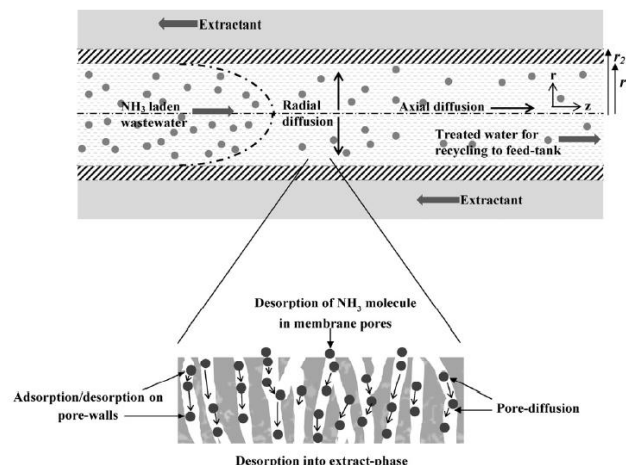


Figure 10. Transport steps for separation of NH_3 molecules through the HFMC (Agrahari et al., 2012)

The first step is radial diffusion of ammonia to the internal surface of hollow fiber and ammonia gas molecules transfer from the aqueous solution to the membrane pores. The second step is the diffusion of ammonia in gaseous form inside the pore. Finally, it reaches the interface located at the pore exit of the hydrophobic membrane and instantaneously reacts with the receiving phase, typically sulphuric acid for ammonia extraction. Ammonia is highly soluble in sulphuric acid present at the shell side. No reaction zone is formed; it reacts only at the interface. This behavior can be seen in Figure 11. (Mandowara and Bhattacharya, 2011)

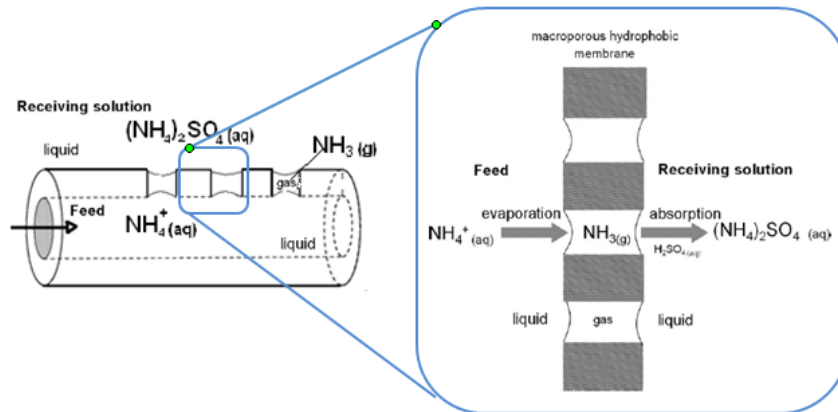


Figure 11. Principle of the extraction process (Hasanoglu et al., 2010)

There are few studies on ammonia removal from wastewater. Zhu et al. (2005) reported a study on the effect of the pH and the viscosity of the wastewater containing ammonia on the mass transfer in hydrophobic hollow fiber membrane contactors. They carried out the experiments at 20°C at different feed solution pH values from 9 to 13 with ammonia concentration varying from 50 to 10000 mg·L⁻¹. They concluded that the removal of ammonia was a function of solution pH, increasing with the increase of pH. When working at high pH the removal was greater. Thus, for a pH above 11 was reached an ammonium removal of 98% in 40 minutes while for pH values of 10 and 9 removal was 60 and 25% respectively in the same period of time. Tan et al. (2006) reported an ammonia removal with the same behavior with the highest extraction at pH=11. The maximum removal of ammonia was achieved above pH 11.

8.2 Mathematical model development for the removal of ammonium from aqueous solution using contactors

8.2.1 Close loop operation mode

Figure 12 shows a schematically set up of close loop operation mode.

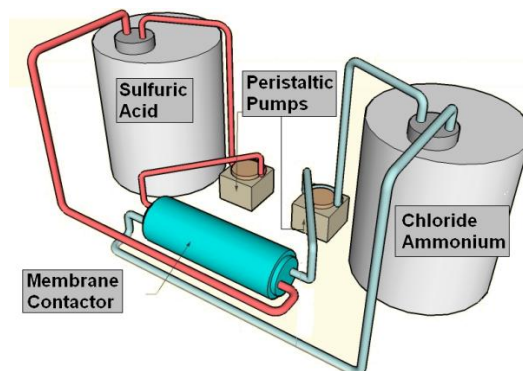


Figure 12. Experimental setup (Lincon et al, 2012)

The hollow fibers modules describe in literature are generally configured in parallel and the gas and liquid flow on the opposite sides of the membrane. The gas phase flowed either outside (shell) or inside (lumen) of the hollow fiber membrane (Mansourizadeh, et al., 2009). Under these conditions the following assumptions have been made by different authors (Mansourizadeh et al., 2009; Rezakazemi et al., 2012; Agrahari et al., 2012; Mandowara and Bhattacharya, 2009; Klaassen et al., 2005) were considered:

- Unsteady state and isothermal conditions.
- Laminar flow for both streams in the hollow fiber membrane contactor (HFMC).
- Henry's law is applicable for feed-membrane interface (thermodynamic equilibrium).
- No pore blockage occurs.
- Non-wetted mode for the membrane is assumed; in which the feed aqueous solution do not fills the membrane pores (since the HFMC is hydrophobic; it prevents passage of feed aqueous solution through the pores).
- There is no reaction zone (the reaction of ammonia with the sulfuric acid is fast (instantaneous) and always occurs in excess).
- Flow rates of both ammonia solution and sulfuric acid are constant.
- Feed tank operates at the perfect mixing mode.

The transport of both ammonia and ammonium ions in the lumen is expressed through a convective-diffusive equation (Mandowara and Bhattacharya, 2009):

$$\frac{\partial C_j}{\partial t} + \tilde{U} \cdot \nabla C_j = D_j \nabla^2 C_j + R_j \quad (\text{Eq. 6})$$

Where

C_j concentration of ammonia and ammonium ions ($\text{mol}\cdot\text{m}^{-3}$)

D diffusivity of the component in water ($\text{m}^2\cdot\text{s}^{-1}$)

R_j rate of generation due to the chemical reaction ($\text{mol}\cdot\text{s}^{-1}\cdot\text{m}^{-3}$)

U velocity vector ($\text{m}\cdot\text{s}^{-1}$)

In this process there is no chemical reaction in the lumen side, so the symmetry assumed inside the lumen is cylindrical (Mandowara and Bhattacharya, 2011):

$$\frac{\partial C_j}{\partial \theta} = 0 \quad (\text{Eq. 7})$$

$$R_j = 0 \quad (\text{Eq. 8})$$

Further, U_r (Radial velocity), which is due to the diffusion of ammonia in the radial direction, also becomes zero. This is because the rate of diffusion of ammonia in water is negligible and the flow is in the Z direction (Mandowara and Bhattacharya, 2009). Now, the equation 6 can be modified as follows:

$$\frac{\partial C_j}{\partial t} + U_z \frac{\partial C_j}{\partial Z} = D_j \left\{ \frac{1}{r} \frac{\partial}{\partial r} \left(r \frac{\partial C_j}{\partial r} \right) + \frac{\partial^2 C_j}{\partial Z^2} \right\} \quad (\text{Eq. 9})$$

Where the velocity distribution in the lumen side under laminar flow conditions can be written (Kreulen et al., 1993) as

$$U_z(r) = 2\bar{U} \left\{ 1 - \left(\frac{r}{R} \right)^2 \right\} \quad (\text{Eq. 10})$$

Where

r radial coordinate (m)

R radius of the lumen (m)

Defining \bar{U} to be the average velocity of the fluid inside the lumen:

$$\bar{U} = \frac{Q}{N\pi R^2} \quad (\text{Eq. 11})$$

Where

\bar{U} average velocity of the fluid inside the lumen ($\text{m}\cdot\text{s}^{-1}$)

Q feed flow rate ($\text{m}^3\cdot\text{s}^{-1}$)

N number of fibers

Once defined the equation governing the mass balance within the lumen, the boundary conditions are:

1. At $r=0$; all Z and t

$$\left(\frac{\partial C_j}{\partial r} \right)_{r=0} = 0 \quad (\text{Eq. 12})$$

2. At $Z=0$; all r and t

$$C_{j,Z=0} = C_{\text{tan } k} \quad (\text{Eq. 13})$$

Equation 13 is related to the fact that this model is based on an unsteady-state situation considering radial and axial diffusion in the lumen; at the entrance, both types of diffusion are neglected (Wehner and Wilhelm, 1956).

3. At $Z=L$; all r and t

$$D_j \left(\frac{\partial^2 C_j}{\partial Z^2} \right)_{Z=L} = 0 \quad (\text{Eq. 14})$$

Equation 14 shows that the diffusion of ammonia at the exit of the lumen (in Z-direction) to be negligible in comparison to its movement in the same direction due to flow.

4. At $r = R$, all Z and t

$$-D_j \left(\frac{\partial C_j}{\partial r} \right)_{r=R} = k_{g,pore} \left(\frac{p_{a,int}^g}{R_g T} \right) \quad (\text{Eq. 15})$$

It can be seen that the flux of ammonia in aqueous phase equals the flux of the gaseous ammonia diffused through the pore as defines equation 15. The concentration of ammonia at the pore exit is assumed to be negligible. This is because an instantaneous reaction between acid and ammonia takes place at the pore exit.

Additionally mass transfer coefficient inside the pore, $k_{g,pore}$ (m/s) can be defined as:

$$k_{g,pore} = D_{a,c,pore} \left\{ \frac{\varepsilon}{\tau b} \right\} \quad (\text{Eq. 16})$$

Where

- $D_{a,c,pore}$ diffusivity of ammonia ($\text{m}^2 \cdot \text{s}^{-1}$)
- ε porosity of the membrane (dimensionless)
- τ tortuosity of the pore (dimensionless)
- b membrane thickness (m)

This correlation was estimated by Mandowara and Battacharya (2009), where the tortuosity is given by (Bottino et al., 2008):

$$\tau = \frac{1}{\varepsilon^2} \quad (\text{Eq. 17})$$

Diffusivity is calculated ($D_{a,c,pore}$) by:

$$\frac{1}{D_{a,c,pore}} = \frac{1}{D_{k,a,pore}} + \frac{1}{D_{a,air}} \quad (\text{Eq. 18})$$

Where

$D_{a,c,pore}$ diffusivity of ammonia in the pore ($m^2 \cdot s^{-1}$)

$D_{k,a,pore}$ Knudsen diffusion ($m^2 \cdot s^{-1}$)

$D_{a,ai}$ diffusivity of ammonia in the air ($m^2 \cdot s^{-1}$)

Further, the Knudsen diffusion $D_{k,a,pore}$ is given by

$$D_{k,a,pore} = \frac{d_{pore}}{3} \left(\frac{8R_g T}{\pi M_a} \right)^{1/2} \quad (\text{Eq. 19})$$

Where

d_{pore} diameter of pore (m)

R_g universal gas constant ($J \cdot mol^{-1} \cdot K^{-1}$)

T temperature (K)

M_a molecular weight of ammonia ($g \cdot mol^{-1}$)

As previously defined, C_j is the concentration of ammonia and ammonium ions ($mol \cdot m^{-3}$):

$$C_j = [NH_3] + [NH_4^+] \quad (\text{Eq. 20})$$

Where

$[NH_3]$ concentration of ammonia ($mol \cdot m^{-3}$)

$[NH_4^+]$ concentration of ammonium ($mol \cdot m^{-3}$)

In the other hand, at the liquid-gas interface located at the pore interface (Figure 13), Henry's law may be applicable (Tan et al., 2006):

$$P_{a,int}^g = H_a \cdot [NH_3]_{int} \quad (\text{Eq. 21})$$

Where

H_a Henry's constant ($Pa \cdot m^3 \cdot mol^{-1}$)

$[NH_3]_{int}$ concentration of ammonia at liquid-gas interface ($mol \cdot m^{-3}$)

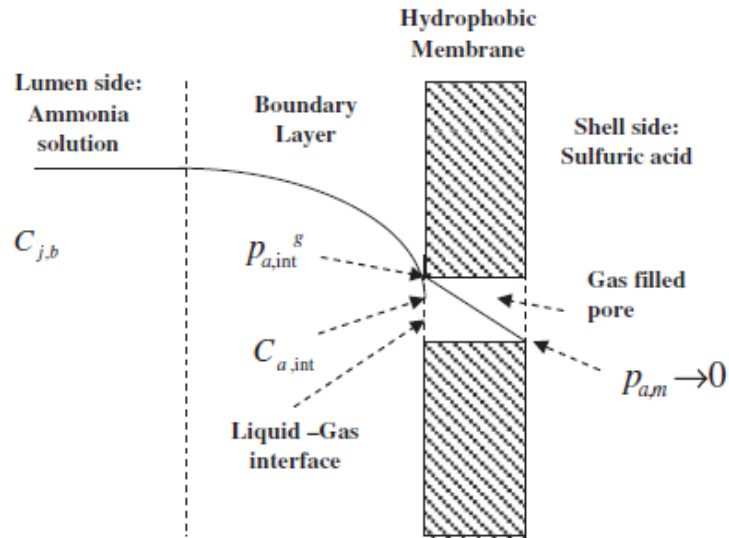


Figure 13. Concentration profile for the species j at a particular time when it moves from lumen side towards shell side through a microporous hydrophobic membrane (Mandowara and Bhattacharya, 2011)

As explained in section 1, in aqueous solution equilibrium is established between dissolved ammonia gas and ammonium ions. A substantial fraction remains in the molecular form in solution.

Under the assumption of uniform mixing, the mass balance equation can be written

$$V \frac{dC_{\text{tank}}}{dt} = QC_{j,Z=L} - QC_{\text{tank}} \quad (\text{Eq. 24})$$

Initial condition: at $t = 0$

$$C_{\text{tank}} = C_0 \quad (\text{Eq. 25})$$

To calculate the fractional removal β of ammonia at time t in the tank:

$$\beta = 1 - \frac{C_{\text{tank}}(t)}{C_0} \quad (\text{Eq. 26})$$

8.2.2 Open loop operation mode

For open loop operation configuration was used the same model but boundary conditions were modified:

1. At steady state in the Eq. 9

$$\frac{\partial C_j}{\partial t} = 0 \quad (\text{Eq. 26})$$

2. At $Z = 0$; all r and t

$$C_{j, Z=0} = C_{\text{tank}} \quad (\text{Eq. 27})$$

In open loop operation mode the initial ammonia concentration is the same that the concentration tank.

9. Objectives and Methodology

9.1 Objectives

The aim of this master project is the elimination of ammonia from the stream entering the Membranes distillation in Greenlysis pilot plant. For this purpose liquid-liquid contactors will be used considering the advantages offered by this technology compared to conventional techniques as has been summarized in state of the art.

The main objective is to investigate and evaluate the hollow fiber membrane contactors performance for ammonia removal from aqueous solutions under different processing conditions and to define the operational parameters necessary to remove ammonia efficiently. The parameters to be evaluated are

- Initial concentrations of the ammonia and sulfuric acid solutions
- the pH of the ammonia feed solution
- the flow-rate feed stream
- Use of different types of water: Tap water, MilliQ and wastewater from the pilot plant.
- Modeling the ammonium removal by membrane contactors by numerical solution of the governing equations.

9.2 Methodology

9.2.1 Reagents

The feeding solution was prepared by dissolving ammonium chloride in 10 L of water for concentrations between 5 and 15 ppm. NaOH solutions were used to achieve pH values higher than the usual value of pK_a and shift the equilibrium to the predominant free molecular NH_3 . To keep constant pH value during all experimental time a borax buffer was used. The receiving solution was prepared dissolving 5 ml of H_2SO_4 98-99% v/v in 5 L of water.

9.2.2 Membrane contactors

A laboratory-scale membrane contactor with polypropylene microporous hollow fibers from Liqui-Cel Company 2.5x8 inch was used. Details on the specifications of this module are collected in Table 3.

Hollow-fiber membrane module	2.5 × 8 Liqui-Cel membrane
Membrane fiber/potting material	Polypropylene/polyethylene
Fiber OD/ID	300/220 μm
Membrane porosity	40%
Liquid flow limits	
Shell side	0.16–1.8 m^3/h
Lumen side	0.1–0.7 m^3/h
Priming volume	
Shell side	0.4 L
Lumen side	0.15 L
Maximum shell side allowable working temperature/pressure	40°C, 7.2 bar
Maximum lumen side allowable working temperature/pressure	70°C, 2.0 bar
Pore diameter	15–25°C, 4.8 bar
Shell side geometric void fraction	0.03 μm
	0.40

Table 3. Specifications of the hollow fiber membrane contactor (Ashrafizadeh, 2010)

Figure 14 shows the internal structure of the membrane contactor.

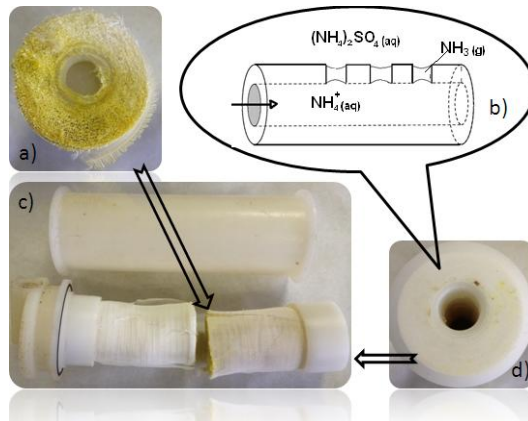


Figure 14. a) Cross section of a membrane module showing the fibers. b) Hollow fiber with the transport phenomena. c) Membrane contactor. d) Side view of the entrance to the hollow fibers. (Licon et al, 2012)

9.2.3 Experimental procedure

The operating conditions of the close and open loop mode have been summarized in Table 4.

Parameter	Interval of values	Unit
Temperature	18-22	°C
Flow rate	0.16-0.26	l/min
pH feed solution	9.27-10.4	-
pH receiving solution	1.88-2	-
Ammonia concentration in the feed	5-25	ppm

Table 4. Operation conditions in the experiments

Experimental configurations:

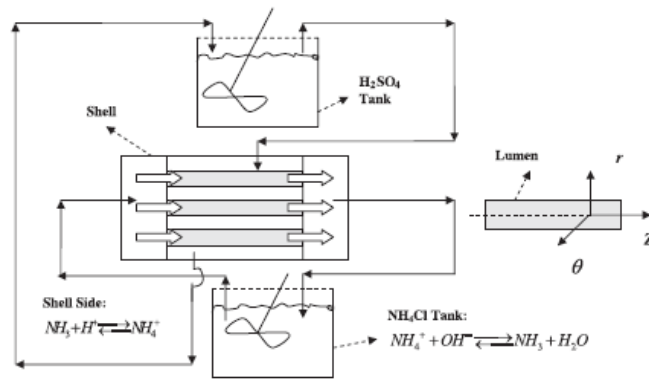


Figure 15. Membrane contactor operated by liquid-liquid extraction (Close loop configuration)
(Mandowara and Bhattacharya, 2011)

Figure 15 shows the setup for ammonia removal in close loop configuration. The ammonia feed solution is pumped through the lumen of the hollow-fiber membrane, while the stripping solution containing sulfuric acid is pumped into the shell side of the hollow-fiber membrane. Both solutions are recycled to their respective reservoirs (Licon et al, 2012)

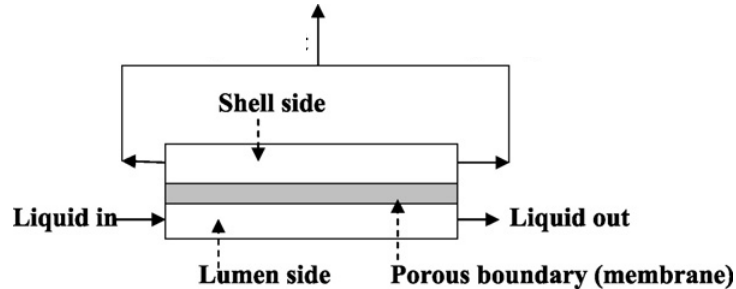


Figure 16. Membrane contactor for the removal of dissolved ammonia (Open loop configuration)
(Mandowara and Bhattacharya, 2009)

Figure 16 shows the setup for ammonia removal in open loop configuration. The process is similar, but the ammonia feed solution is not recycled.

At the end of the experiment, the shell-side flow and the tube-side flow were stopped. The system was properly shut down and thoroughly cleaned by passing deionized water through both sides to remove the remaining solution.

9.2.4 Monitoring protocol

The procedure for sampling in closed circuit was as follows:

1. At regular time intervals (10 minutes) 5mL samples were taken from the tank of feed solution. In total, 18 samples were collected by each experiment..
2. The pH was measured by pH meter GLP22 Crison, Spain.
3. The samples were prepared for determined the ammonia concentration by ion exchange chromatography.

The procedure for sampling in open circuit was as follows:

1. For the first experiments in open loop configuration, samples were taken every 5 minutes, obtaining 21 samples for each experiment. Once evolution was determined, the samples were taken every 10 minutes, reducing the number of samples to 10-13 for experiment depending on the flow rate.
2. The pH was measured by pH meter GLP22 Crison, Spain.
3. The samples were prepared for determined the ammonia concentration by ion exchange chromatography.

All the experimental conditions are summarized in the Table 5.

	Experiment	Conditions								
		Tank Volume (L)		pH in tank		Flow rate (l/min)	[NH ₄ ⁺] (ppm)	Type of circuit	Buffer	NaOH 2M
		H ₂ SO ₄	NH ₄ ⁺	H ₂ SO ₄	NH ₄ ⁺					
Tap water	1	5	10	2	7,3	0,26	8	Closed loop	No	No
	2	5	10	2	10,4	0,26	5	Closed loop	Yes	Yes
	3	5	10	1,88	9,2	0,26	15	Closed loop	No	Yes
	4	5	10	1,97	10,4	0,26	15	Closed loop	Yes	Yes
	5	5	10	2,06	9,8	0,26	15	Closed loop	Yes	Yes
	6	5	10	1,88	10,1	0,26	15	Closed loop	Yes	Yes
	7	5	10	1,86	10,1	0,61	15	Closed loop	Yes	Yes
Deionized Water	8	10	25	1,92	9,9	0,26	5	Open loop	No	Yes
	9	10	25	1,85	10,5	0,26	5	Open loop	No	Yes
	10	10	25	1,95	9,9	0,41	5	Open loop	No	Yes
	11	10	25	1,9	9,9	0,15	5	Open loop	No	Yes
	12	10	25	1,81	9,9	0,26	10	Open loop	No	Yes
	13	10	25	1,83	9,5	0,26	10	Open loop	No	Yes
Wastewater	14	10	25	1,82	9,8	0,26	7,8	Open loop	No	Yes
	15	10	25	1,89	9,8	0,26	12,3	Open loop	No	Yes
	16	10	25	1,77	9,8	0,26	24,3	Open loop	No	Yes

Table 5. Summary of the experiments at conditions evaluated

10. Results and discussion

The evolution of the different parameters evaluated on each experiment is collected in Annex 1. The quantification of the efficiency (% removal NH_4^+) of the liquid-liquid membrane contactors on ammonia removal was calculated by using equation 28:

$$\% \text{ removal}(\text{NH}_4^+) = \frac{C_{\text{NH}_4^+(t=0)} - C_{\text{NH}_4^+(t)}}{C_{\text{NH}_4^+(t=0)}} \cdot 100 \quad (\text{Eq. 28})$$

Where

$C_{\text{NH}_4^+(t=0)}$ is the total ammonium concentration at $t=0$

$C_{\text{NH}_4^+(t)}$ is the total ammonium concentration at time (t)

Simulation studies were carried out for the removal of ammonia from water via membrane contactor using COMSOL software. In section 8 the model equations were explained for close and open loop configuration. For both modes, was used the equation 9 for describes the mass balance inside the lumen and using different boundary conditions for each type of circuit. Table 6 collects the mass transfer equation (equation 5) and the boundary conditions for close and open loop configuration:

Mass transfer equation	$\frac{\partial C_j}{\partial t} + U_z \frac{\partial C_j}{\partial Z} = D_j \left\{ \frac{1}{r} \frac{\partial}{\partial r} \left(r \frac{\partial C_j}{\partial r} \right) + \frac{\partial^2 C_j}{\partial Z^2} \right\}$	
Boundary conditions	Close loop configuration	Open loop configuration
	$\left(\frac{\partial C_j}{\partial r} \right)_{r=0} = 0$	$\frac{\partial C_j}{\partial t} = 0$
	$C_{j,Z=0} = C_{\tan k}$	$C_{j,Z=0} = C_{\tan k}$
	$D_j \left(\frac{\partial^2 C_j}{\partial Z^2} \right)_{Z=L} = 0$	
	$-D_j \left(\frac{\partial C_j}{\partial r} \right)_{r=R} = k_{g,pore} \left(\frac{p_{a,int}^g}{R_g T} \right)$	

Table 6. Model equations and boundary conditions

The mathematical model and the experimental results enabled to obtain the next characteristics parameters of the membrane.

- Inner radius of the lumen, d_i (m)
- Length of the fiber, L (m)
- Diffusivity of ammonia, $D_{a,air}$ (m^2/s)
- Diffusivity in water, D_j (m^2/s)
- Dissociation constant of ammonia, K_b

It has been used the values stated in Mandowara (2011) as initial values to perform the non-linear least squares method in order to estimate them, since the experimental module and close loop configuration is the same used in the presented study. Table 7 shows the nominal values of these parameters. Then the diffusion coefficient ($D_{a,c,pore}$) and mass transfer coefficient ($k_{a,g,pore}$) were calculated with the obtained data by the equations 16-19.

Parameter	Value
Inner radius of the lumen, d_i (m)	$1.1 \cdot 10^{-4}$
Length of the fibre, L (m)	0,2
Diffusivity in water, D_j (m^2/s)	$1.76 \cdot 10^{-9}$
Diffusivity in air, $D_{a,air}$ (m^2/s)	$1.89 \cdot 10^{-5}$
Dissociation constant of ammonia, K_b	$1.744 \cdot 10^{-5}$

Table 7. Initial values of parameters to be estimated

Furthermore, other required parameters were taken from the membrane contactor manufacturer and Mandowara (2011) they can be seen in Table 8.

	Parameter	Nominal value
Membrane contactor manufacturer	Thickness of the membrane, b (m)	$3 \cdot 10^{-5}$
	Pore diameter, d_{pore} (m)	$4 \cdot 10^{-8}$
	Porosity, ϵ	0,4
	Number of fibers, N	10000
Mandowara, 2011	Kinematic viscosity of water at $T=298^{\circ}\text{K}$, η (m^2/s)	$1 \cdot 10^{-6}$
	Henry's law constant, H_a ($\text{Pa} \cdot \text{m}^3/\text{mol}$)	1,62

Table 8. Nominal values of membrane contactor parameters

For the open loop configuration, the simulation was started with the estimated values obtained in close loop configuration. The mathematical model is the same that close loop configuration but the boundary conditions are different. In this case, only a value of the experimental result is compare with the model. This value corresponds to the concentration at the outlet of the membrane contactor at the end of the experiment.

On the other hand, the model defined allowed to compare the experimental results obtained in both cases to observe the influence of the operational parameters (pH, flow rate and initial concentration of ammonium) for each stage.

To estimate the accuracy between the experimental data and the model prediction data and statistical parameter was used, the root-mean-square deviation (RMSD). The root-mean-square deviation (RMSD) for the experiments of close and open loop configuration is calculated by following equation:

$$RMSD = \sqrt{\frac{\sum_{i=1}^n (C_{\text{est},i} - C_{\text{exp},i})^2}{n}} \cdot 100 \quad (\text{Eq. 29})$$

10.1 Results and discussion for close loop operation mode

The experiments performed in closed loop configuration were performed by using tap water and most of these experiments were carried out in order to optimize the experimental conditions for close loop configuration.

The effect of the feed solution pH was evaluated at pH ranged from 9.3 to 10.4. The ammonium removal was observed at pH values below the pKa as can be seen in Figure 17. The experiment performed at pH 9.3 observed a low (10%) removal efficiency compared to higher removals obtained for the experiments at pH 10.4 and 10.1 with removals above 90%. Then, the following experiments were carried out at pH values above pKa.

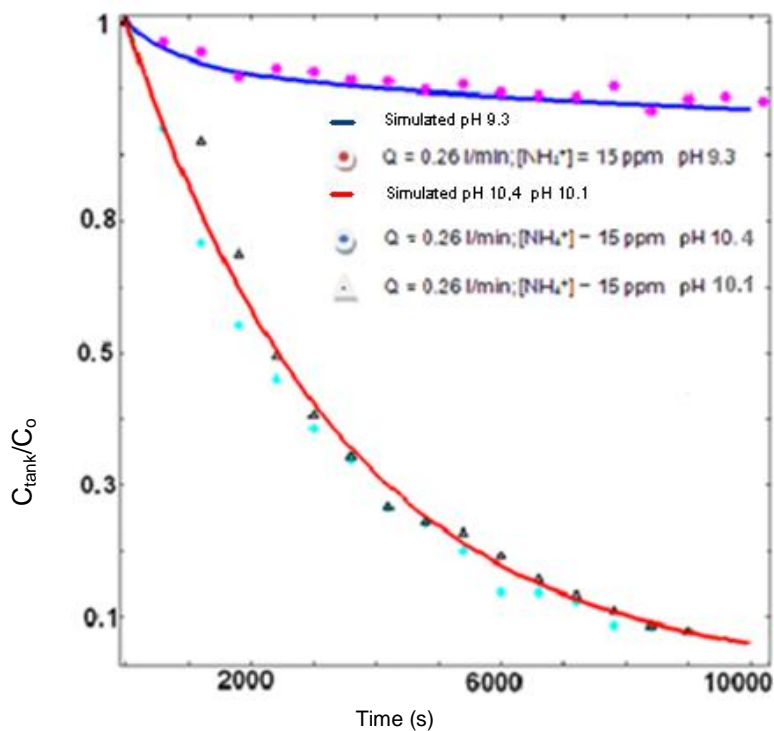


Figure 17. Influence of feed solution pH on the fractional removal in the close loop configuration, with flow rate 0.26 l/min and initial ammonium concentration of 15 ppm. Comparison between simulated values and experimental data.

Table 9 shows the influence of the pH in the ammonia removal process. In values above pH=10 the removal efficiency is higher than 99%. The increases of pH increases the percentage of the NH_3 in the aqueous feed solution concentration as could be seen in section 4.1 (Figure 2). The root-mean-square deviations (RMSD) determine the agreement between the mathematical model and the experimental data. The values observed were below 6% indicating the good fitting of the experimental data to the mathematical model.

Flow rate (l/min)	[NH ₄ ⁺] (ppm)	Type of circuit		
0.26	15	Close loop		
Experiment	pH (NH ₄ ⁺)	% Removal	Removal Time (min)	RMSD (%)
3	9.3	15	180	1.37
4	10.4	100	140	3.47
6	10.1	100	150	5.39

Table 9. Experimental results and RMSD with variable pH in close loop configuration with flow rate 0.26 l/min and initial concentration of ammonium of 15 ppm

The effect of initial ammonium feed concentration varying from 5 to 15 mg/l at pH 10.4 and flow rate 0.26 l/min as can be seen in Figure 18. It is observed that the initial concentration of ammonium did not affect the ammonium removal in the membrane contactor.

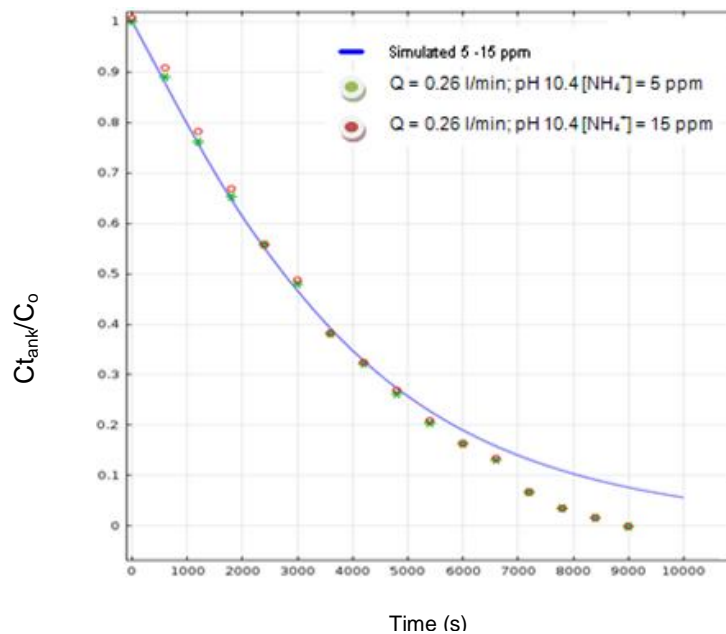


Figure 18. Influence of initial ammonium concentration in fractional removal in the close loop configuration with flow rate 0.26 l/min and pH 10.4. Comparison between simulated values and experimental data.

The initial concentration of ammonia is a parameter that not has influences in the removal process. This behavior is predicted by the fact that the diffusivity coefficient is a weak function of ammonia concentration, especially in the dilute range. The resistance offered by the overall process to the ammonia removal becomes independent of the initial ammonia concentration. The small difference that can be observed in Figure 18 between the experimental and predicted values is probably due to the evaporation of ammonia from the feed tank during the experimentation.

Table 10 shows the experimental conditions and the results of the influence of initial concentration in the ammonium removal. It is observed that NH_4^+ concentration in the aqueous feed is not an influence factor in the ammonium removal process. In Table 10 can be seen the deviation between the experimental data with the mathematical model (<5%).

Flow rate (l/min)	pH (NH_4^+)	Type of circuit		
0.26	10.4	Close loop		
Experiment	$[\text{NH}_4^+]$ (ppm)	% Removal	Removal Time (min)	RMSD (%)
2	5	100	150	4.10
4	15	100	150	3.80

Table 10. Experimental results and RMSD with variable initial concentration in close loop configuration with flow rate 0.26 l/min and pH 10.4

Finally, in order to determine the influence of flow rate in the ammonia removal in a close loop configuration a comparison of simulation and experimental results is reported in Figure 19. The experiments had been carried out with initial concentration of ammonium of 15 ppm and pH 10.1. The flow rate had been varied from 0.26 l/min to 0.61 l/min. It is observed that this parameter has strong influence in the removal ammonium time. When increases the flow rate the removal time decreases.

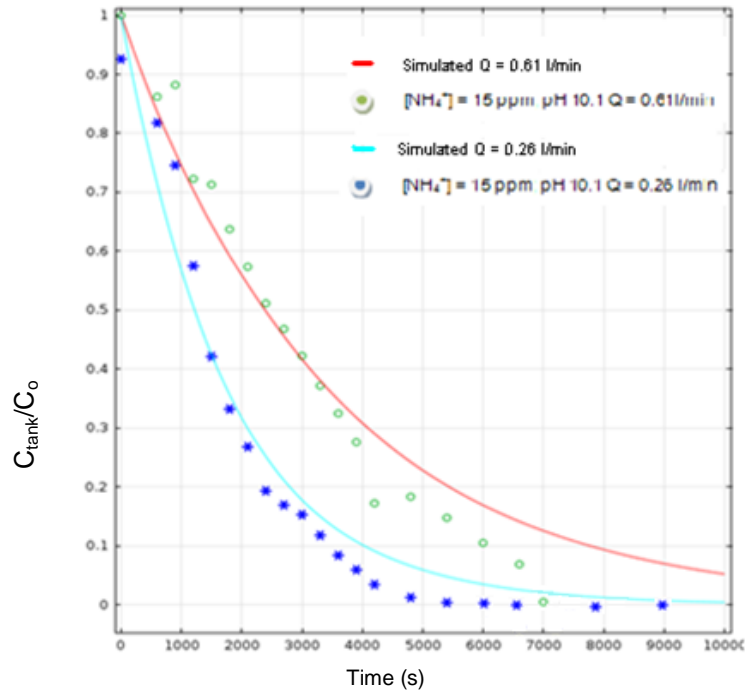


Figure 19. . Influence of flow rate on the fractional removal in the close loop configuration with Initial concentration of ammonium 15 ppm and pH 10.1. Comparison between simulated values and experimental data.

The strong influence of the flow rate in the ammonium removal can be explained since an increase on the flow rate represents an increase on the convection in the lumen side, then the viscous layer resistance decreased near the wall of the fiber and ammonia removal is faster.

The experimental conditions of these experiments in order to determine the influence of flow rate in fractional ammonium removal are summarized in Table 11. It shows that increases of the feed flow rate maintain the removal efficiency for 15 mg/l solutions and reduce the contact time required from 150 to 120 minutes to achieve a quantitative removal of ammonium. The values of RMSD (<7%) shows the agreement the experimental data with the mathematical model.

$[\text{NH}_4^+]$ (ppm)	pH (NH_4^+)	Type of circuit		
15	10.1	Close loop		
Experiment	Flow rate (l/min)	% Removal	Removal Time (min)	RMSD (%)
6	0.26	100	150	5.60
7	0.61	100	120	6.80

Table 11. Experimental results and RMSD with variable flow rate in close loop configuration with initial concentration of ammonium of 15 ppm and pH 10.1

According to the obtained results it is possible to define the optimal experimental conditions for ammonium removal in close loop configuration. These conditions are summarized in Table 12.

Close loop configuration	pH [NH_4^+]	Flow rate (l/min)
Optimal conditions	>9.3 <10.5	0.61

Table 12. Optimal work conditions in close loop configuration

All experiments of close loop configuration are summarized in the Annex 2.

10.2 Results and discussion for open loop operation mode

Based on the results obtained in closed circuit experiments, in open loop configuration were performed in order to evaluate the influence of pH, initial concentration and flow rate in the ammonium removal.

The experiments in open loop configuration were performed by using deionized water and wastewater from the pilot plant. The most of the experiments with deionized water were performed in order to optimize the experimental conditions in open loop configuration. Then, considering these conditions were carried out the experimental with wastewater from the plant to achieve maximum ammonium removal.

- **Experiment results by using Deionized water**

The first parameter studied in open loop configuration was the influence of feed solution pH. In close loop configuration, it was observed that when it was worked with a pH values below the pKa the removal efficiency was lower. So in the experiments in open loop were worked with a pH values over the pKa. It was evaluated the influence of this parameter in the range of pH from 9.9 to 10.5. Both experiments performed with a pH value over the pKa and it was observed removal efficiencies above the 90%. Then, the following experiments were carried out at pH values from 9.5 - 10, considering that for pH values above 10 the elimination is similar than pH values under 10 as can be seen in Figure 20.

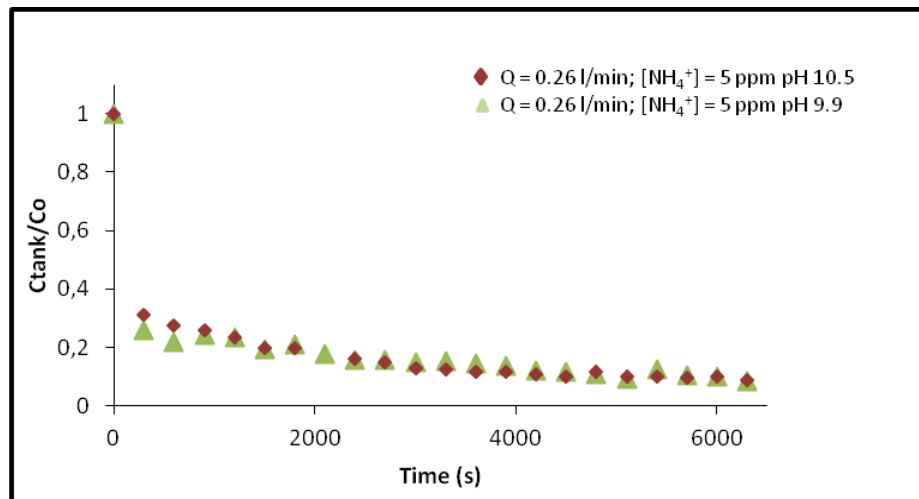


Figure 20. Influence of feed solution pH on the variation in fractional removal in the open loop configuration with $Q = 0.26$ l/min and initial concentration of ammonium 5 ppm. Experimental values

The experimental conditions and the results in open loop configuration with flow rate (0.26 l/min) and ammonia concentration (5 mg/l) removal ratio of ammonium achieved values of 91-92 % as can be seen in Table 13. The root-mean-square deviation (RMSD) which can be seen in Table 13 belongs to the experimental data deviate from the mathematical model for the experiments compared.

Flow rate (l/min)	[NH ₄ ⁺] (ppm)	Type of circuit		
0.26	5	Open loop		
Experiment	pH (NH ₄ ⁺)	% Removal	Removal Time (min)	RMSD (%)
8	9.9	92	105	2.70
9	10.5	91	105	

Table 13. Experimental results and RMSD with variable pH in open loop configuration with flow rate 0.26 l/min and initial concentration of ammonium 5 ppm

The influence of flow rate in the ammonium removal efficiency in open loop configuration is shown in Figure 21. The experiments were performed with pH 9.9 and initial concentration of ammonia of 5 ppm. The behavior observed was the decreases ammonia removal when the flow rate increases. This is due to increment of residential time inside the membrane contactor.

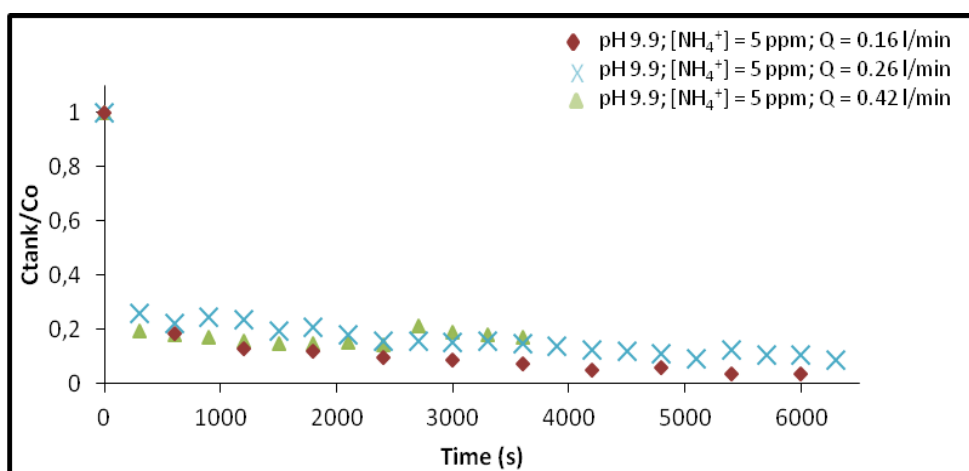


Figure 21. Influence of flow rate on the variation in fractional removal in the open loop configuration with pH 9.9 and initial concentration of ammonium 5 ppm. Experimental values

Figure 22 shows the concentration at the outlet of the membrane contactor at the end of the experiment and the mathematical model. It can be seen that the model prediction fit properly the experimental data. However and slightly deviation was observed at in higher flow rates.

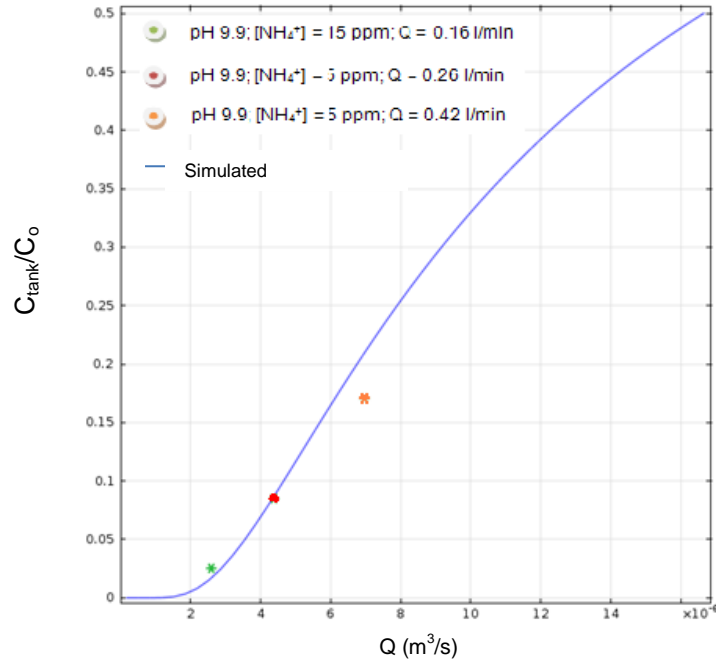


Figure 22. Influence of flow rate on the variation in fractional removal in the open loop configuration with pH 9.9 and initial concentration of ammonium 5 ppm. Comparison between simulated values and experimental data.

Table 14 collects the experimental conditions and the results in open loop configuration when flow rate varies when pH (9.9) and ammonia initial concentration (5 mg/l) were kept constant. The removal ratio of ammonium achieved values around 98 % for the lowest flow rate and 83% for the maximum. The deviation respect to the model is lower than 5%.

pH (NH ₄ ⁺)	[NH ₄ ⁺] (ppm)	Type of circuit		
9.9	5	Open loop		
Experiment	Flow rate (l/min)	% Removal	Removal Time (min)	RMSD (%)
11	0.16	98	100	2.29
8	0.26	92	105	
10	0.42	83	60	

Table 14. Experimental results and RMSD with variable flow rate in open loop configuration with initial concentration of ammonium of 5 ppm and pH 9.9

The influence of initial concentration of ammonium has been seen in Figure 23. The experiments have been performed with a constant flow rate (0.26 l/min) and pH of 9.9. The experimental results of higher initial concentration of ammonium does not show a clear tendency, but it was observed at the end of the experiment that the removal efficiency is higher (92%) for the 5 ppm of initial concentration. Then, in open loop configuration, the influence of the initial concentration in the removal **process** is a key parameter to be considered.

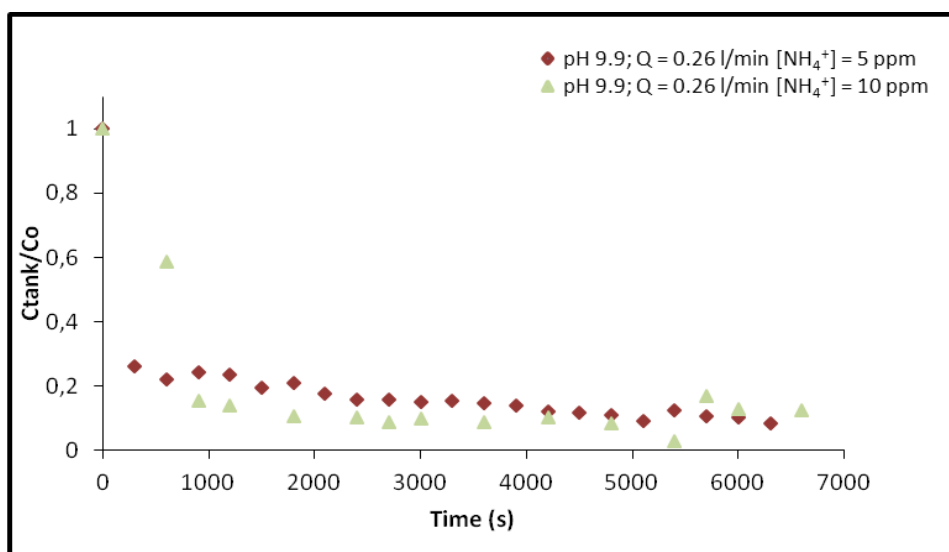


Figure 23. Influence of initial concentration on the variation in fractional removal in the open loop configuration with pH 9.9 and Q = 0.26 l/min. Experimental values

The increase of concentration from 5 mg/l to 10 mg/l at constant pH and flow rate decreases the removal efficiency from 92% to 88% as can be seen in Table 15. The root-mean-square deviations (RMSD) which also are summarized in Table 15 showed values below 5% which indicates that model prediction fit properly the experimental data.

pH (NH ₄ ⁺)	Flow rate (l/min)	Type of circuit		
9.9	0.26	Open loop		
Experiment	[NH ₄ ⁺] (ppm)	% Removal	Removal Time (min)	RMSD (%)
8	5	92	105	3.04
12	10	88	110	

Table 15. Experimental results and RMSD with variable initial concentration of ammonium in open loop configuration

The optimal parameters for ammonium removal in open loop configuration it can be seen in Table 16.

Open loop configuration	pH [NH ₄ ⁺]	Flow rate (l/min)
Optimal conditions	>9.3 <10	0.16

Table 16. Optimal work conditions in open loop configuration

As was observed in open loop configuration, the optimum pH value should be above the pKa. On the other hand, the flow rate, in this case, should be below compared to close loop configuration, in order to increase the residence time and then the removal of ammonium is favored.

- **Experiment results by using Wastewater**

Once the optimal parameters for the efficiency of ammonium removal were determined the pilot plant wastewater was used in the following experiments. The pH of the feed solution was the optimum (9.3 - 10), while the flow used was 0.26 l/min although the optimum flow is lower, the difference in the removal of ammonium was not significant as reported in Figure 24 and additionally the experimental time is reduced. The parameter evaluated in these experiments was the initial concentration of ammonia, which is a requirement from the pilot plant operation and it is due to the variability in the concentration of different substances in solution which depends on several parameters (operating, season, etc.).

The ammonium concentration in the outlet stream as a function of time with initial feed concentration varying from 7.8-24.3 mg/l is shown in Figure 24. For the same initial volume (25 l), ammonia removal decreases with the ammonia concentration increases.

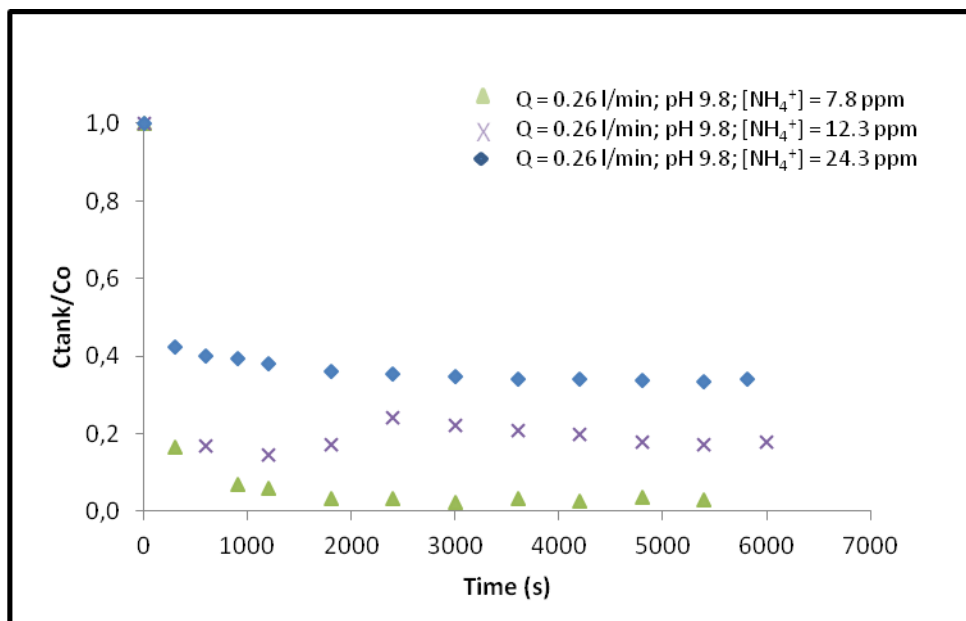


Figure 24. Influence of initial concentration on the variation in fractional removal in the open loop configuration with wastewater with $Q = 0.26$ l/min and pH 9.8. Experimental values

The concentration at the outlet of the membrane contactor at the end of the experiment and the mathematical model prediction are shown in Figure 25. It can be observed that model description is quite good when compared to the experimental data and a slightly deviation is observed at higher flow rate as was observed previously in section 10.1. The general deviation of this parameter can be seen in Table 17.

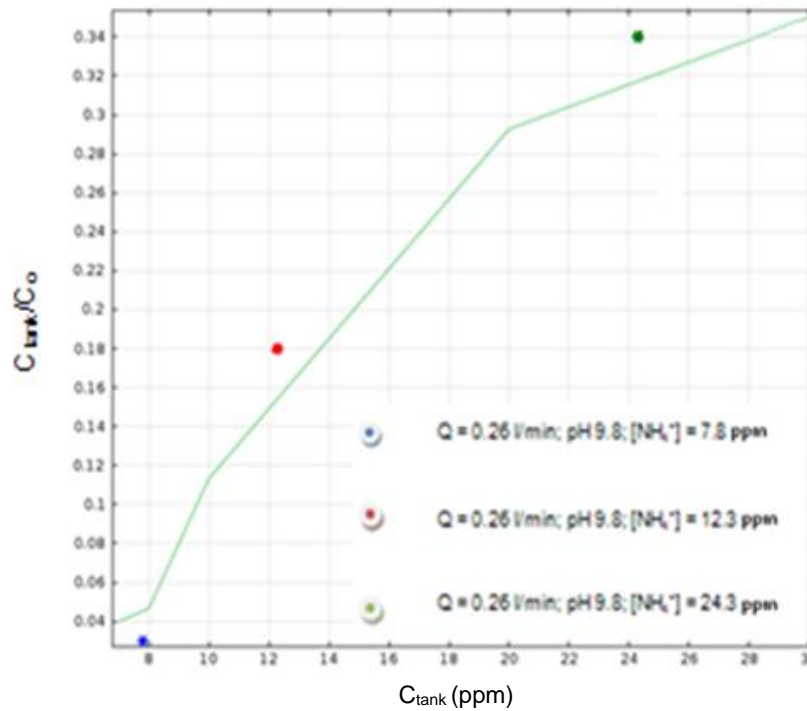


Figure 25. Influence of flow rate on the variation in fractional removal in open loop configuration with $Q = 0.26$ l/min and pH 9.8. Comparison between simulated values and experimental data.

Table 17 shows the experimental conditions and the results of the experiments with wastewater. The increase of concentration from 7.8 mg/l to 24.3 mg/l at constant pH and flow rate decreases the removal efficiency from 97% to 66%. The deviation with the mathematical model is >5%. One reason may be the existence of other species in solution because it was worked wastewater from the plant and the mathematical model was designed for the deionized water.

pH (NH ₄ ⁺)	Flow rate (l/min)	Type of circuit		
9.8	0.26	Open loop		
Experiment	[NH ₄ ⁺] (ppm)	% Removal	Removal Time (min)	RMSD (%)
14	7.8	97	90	7.80
15	12.3	82	100	
16	24.3	66	97	

Table 17. Experimental results and RMSD with variable initial concentration of ammonium in open loop configuration with wastewater

All experimental results of open loop configuration can be seen in the Annex 2.

Finally, it is shown in Table 19 the diffusivity coefficient in the pore ($D_{a, c, \text{pore}}$) and the mass transfer coefficient were calculated with equations 16-19 using the estimated parameters obtained by non-linear least squares method for close and open loop configuration (Table 18).

	Close loop	Open loop
Inner radius of the lumen, d_i (m)	$1.18 \cdot 10^{-04}$	$1.23 \cdot 10^{-4}$
Length of the fibre, L (m)	0.178	0.180
Diffusivity in water, D_j (m ² /s)	$2.06 \cdot 10^{-09}$	$2.12 \cdot 10^{-9}$
Diffusivity in air, $D_{a, \text{air}}$ (m ² /s)	$1.92 \cdot 10^{-05}$	$2.05 \cdot 10^{-5}$
Dissociation constant of ammonia, K_b	$1.64 \cdot 10^{-05}$	$1.735 \cdot 10^{-5}$

Table 18. Parameters estimated for close and open loop configuration model

	Close loop	Open loop
Diffusivity coefficient, $D_{a, c, \text{pore}}$ (m²/s)	$3.56 \cdot 10^{-6}$	$3.74 \cdot 10^{-6}$
Mass transfer coefficient, $k_{g, \text{pore}}$ (m/s)	$7.59 \cdot 10^{-3}$	$9.25 \cdot 10^{-3}$

Table 19. Characteristics parameters for close and open loop configuration model

11. Conclusions

The experiments results obtained with close loop configuration indicate that the optimum pH values for operation must be above the pKa ($\text{NH}_3 / \text{NH}_4^+$). For this pH values removal is quantitative (>99%). On the other hand, when working with a pH below the pKa, the removal efficiency of the process decreases below to 10-15% even for low flow rates. For this reason, the use of a buffer solution is required to keep the pH and additives of small amount of a strong base as NaOH will be enough to achieve these buffering conditions.

Other parameter that was studied is the initial concentration of ammonium in the feed solution. Increasing the initial concentration does not show influence in the removal efficiency, however it is increased the time to achieve the quantitative removal.

From the point of view of the flow rate, when this parameter was increased, the removal efficiency was not affected and the time to reach quantitative removal of ammonium was reduced.

In open loop configuration, experiments showed that the pH feed solution must be above the pKa, but in this cases, the use so concentrate buffer solutions is not required. Removal efficiency of ammonium reached values around 90-92%. An increase of the initial ammonium concentration represents a decrease in the ammonium removal efficiency.

Finally, the maximum removal efficiency in open loop configuration was obtained when pH is above the pKa in a solution and the flow rate is maintained as low as possible.

The proposed model can describe properly the experimental data, especially in close loop configuration and some deviation were observed in open loop configuration. However it can be considered a powerful tool to predict the ammonium removal by membrane contactors under different experimental conditions.

Due to obtained results, the use of liquid-liquid membrane contactor technology can be a good alternative to solve the problem of the conductivity in the electrolysis process within the European project Greenlysis "Hydrogen and Oxygen production by electrolysis via renewable energies to reduce environmental footprint of a waste water treatment plant (WWTP)."

12. Annex

12.1 Annex 1. Summary of the experimental results

12.2 Annex 2. Graphics of experimental results

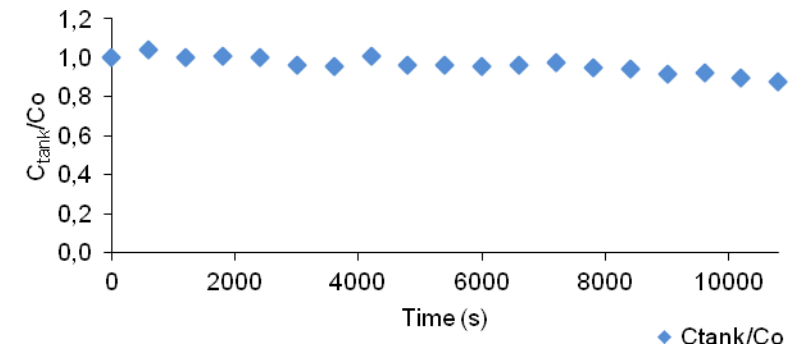
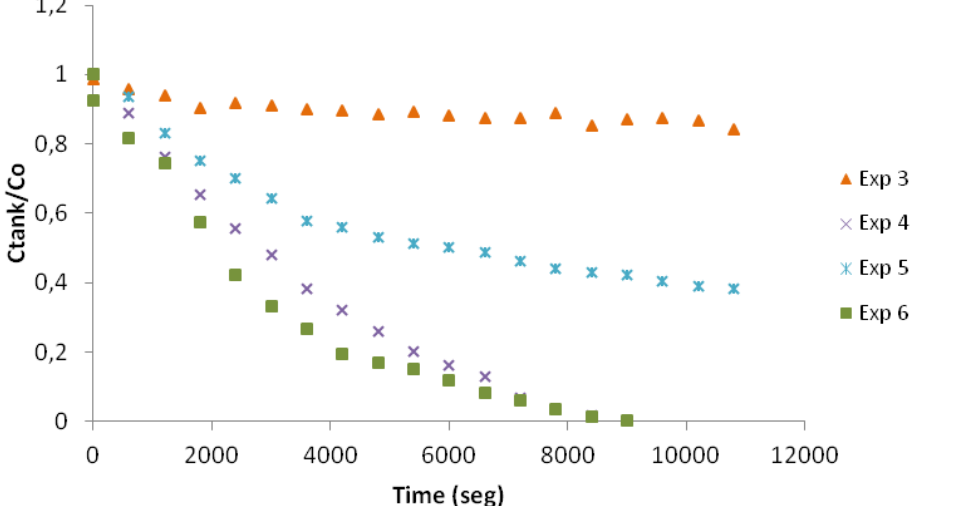
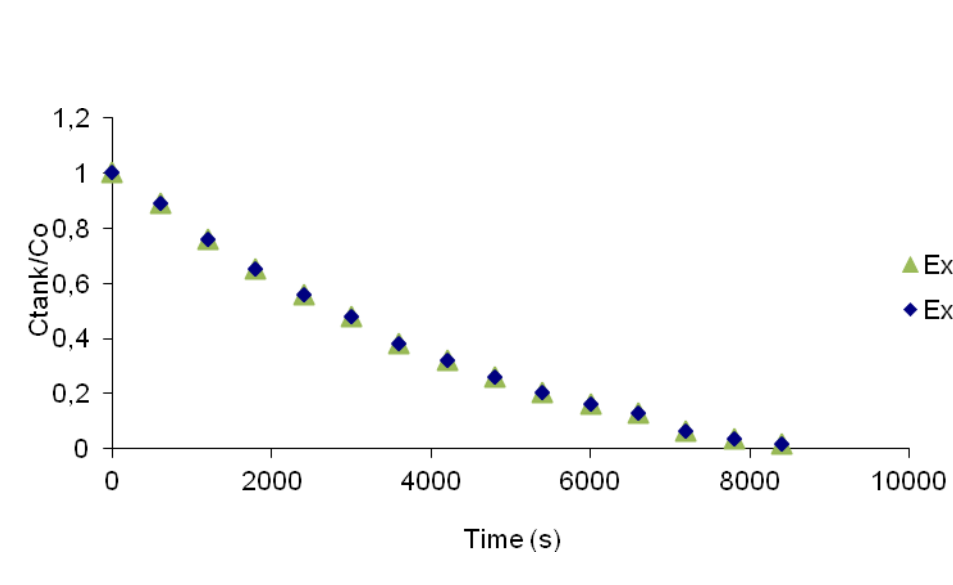
12.3 Annex 3. Poster exhibited in Milan COMSOL Congress in October 2012

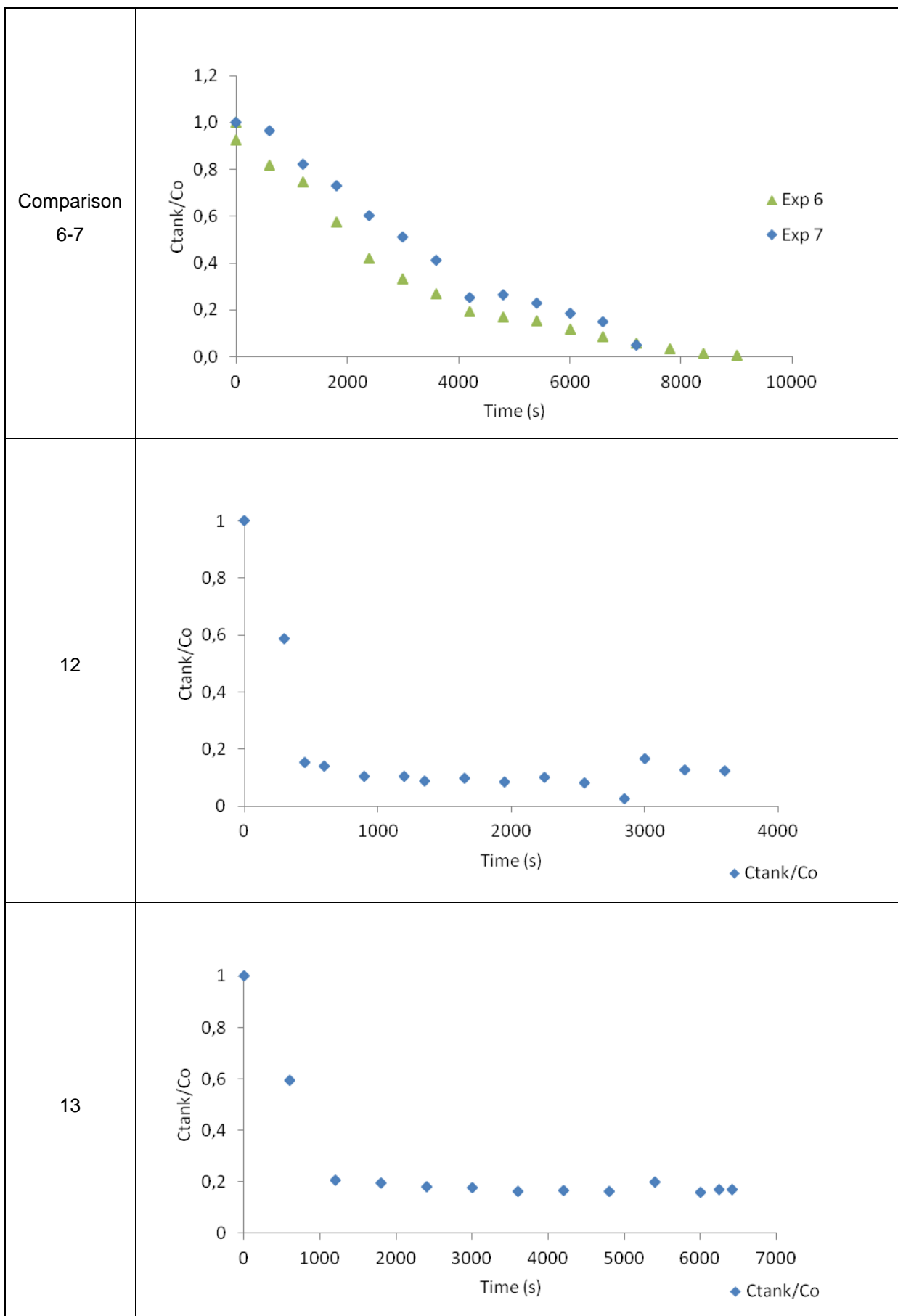
12.4 Annex 4. Paper exhibited in Milan COMSOL Congress in October 2012

12.1 Annex 1. Summary of the experimental results

	Experiment	Conditions									% Removal	Removal Time (min)
		Tank Volume (L)		pH in tank		Flow rate (l/min)	[NH ₄ ⁺] (ppm)	Type of circuit	Buffer	NaOH 2M		
		H ₂ SO ₄	NH ₄ ⁺	H ₂ SO ₄	NH ₄ ⁺							
Tap water	1	5	10	2	7,3	0,26	8	Closed loop	No	No	12,5	180
	2	5	10	2	10,4	0,26	5	Closed loop	Yes	Yes	100	150
	3	5	10	1,88	9,2	0,26	15	Closed loop	No	Yes	15	180
	4	5	10	1,97	10,4	0,26	15	Closed loop	Yes	Yes	100	140
	5	5	10	2,06	9,8	0,26	15	Closed loop	Yes	Yes	61,7	180
	6	5	10	1,88	10,1	0,26	15	Closed loop	Yes	Yes	100	150
	7	5	10	1,86	10,1	0,61	15	Closed loop	Yes	Yes	100	120
Deionized Water	8	10	25	1,92	9,9	0,26	5	Open loop	No	Yes	92	105
	9	10	25	1,85	10,5	0,26	5	Open loop	No	Yes	92	105
	10	10	25	1,95	9,9	0,41	5	Open loop	No	Yes	83	60
	11	10	25	1,9	9,9	0,15	5	Open loop	No	Yes	98	100
	12	10	25	1,81	9,9	0,26	10	Open loop	No	Yes	88	110
	13	10	25	1,83	9,5	0,26	10	Open loop	No	Yes	83	107
Wastewater	14	10	25	1,82	9,8	0,26	7,8	Open loop	No	Yes	97	90
	15	10	25	1,89	9,8	0,26	12,3	Open loop	No	Yes	82	100
	16	10	25	1,77	9,8	0,26	24,3	Open loop	No	Yes	66	97

12.2 Annex 2. Graphics of experimental results

Experiment	Graphics
1	 <p>A scatter plot showing the ratio C_{tank}/C_o on the y-axis (ranging from 0.0 to 1.2) against Time (s) on the x-axis (ranging from 0 to 10,000). The data points, represented by blue diamonds, are consistently plotted at a value of 1.0 across the entire time range.</p>
Comparison 3-6	 <p>A scatter plot comparing four experiments. The y-axis is C_{tank}/C_o (0.0 to 1.2) and the x-axis is Time (seg) (0 to 12,000). Exp 3 (orange triangles) remains constant at 1.0. Exp 4 (purple crosses) decreases to ~0.15 at 6,000s. Exp 5 (light blue crosses) decreases to ~0.4 at 10,000s. Exp 6 (green squares) decreases to 0 by 8,000s.</p>
Comparison 2,4	 <p>A scatter plot comparing two experiments. The y-axis is C_{tank}/C_o (0.0 to 1.2) and the x-axis is Time (s) (0 to 10,000). Both Exp 2 (blue diamonds) and Exp 4 (green triangles) show a very similar decreasing trend, reaching 0 by approximately 8,000 seconds.</p>



12.3 Annex 3. Poster exhibited in Milan COMSOL Congress in October 2012

Ammonia Removal from Water by Liquid-Liquid Membrane Contactor under Closed Loop Regime. ¹

Edxon. E. Licon*¹, Aurora Alcaraz¹, Sandra Casas¹, Jose L. Cortina¹, Cesar A. Valderrama¹

¹Universitat Politècnica de Catalunya, Chemical Engineering Department, Av. Diagonal 647, Barcelona, Spain 08028.

Introduction: This work study how to remove ammonium by a liquid-liquid membrane contactor from water of a waste water treatment plant, This technology will be applied in the Hydrogen and Oxygen production by electrolysis via renewable energies (Figure 1).

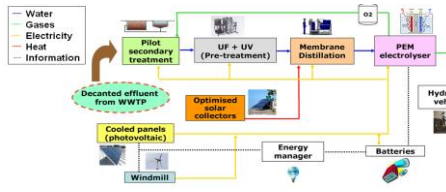


Figure 1. Outline of the Greenlysis project.

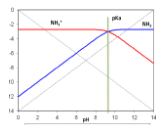
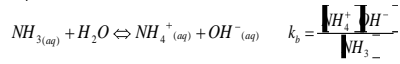


Figure 2. Ammonia equilibrium in water at different values of pH. Ammonia in water exists in free and ionic forms under equilibrium.



Experimental: The feed was delivered inside the hollow fiber (lumen) with different flow rates from a 10L tank containing aqueous NH₄⁺ solution and was continuously recycled. In the other hand, the acid solution contained in a 5 L tank was delivered in the outside of the fibers inside the HFMC (shell) at constant flow rate in a countercurrent mode and was continuously recycled (Figure 3 and 4).

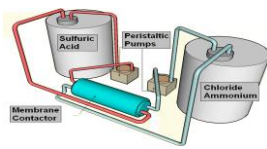


Figure 3. Experimental Setup.

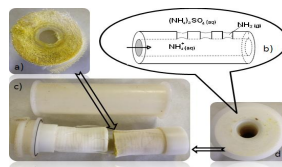


Figure 4. Schematic representation of the transport phenomena occurring inside the hollow fiber.

Computational Methods: One single hollow fiber is simulated using a 2D axisymmetric model (Figure 4). The model equations were developed considering radial and axial diffusion and convection in the lumen with laminar flow conditions (Figure 5-a) and nondimensionalized only in terms of the aspect ratio of the hollow fibers in order to solve them using the PDE coefficient form (Figure 5-c). The recirculation is taken into account as a boundary condition, where a global equation that describes the concentration in the tank is solved (Figure 5-b).

$$\frac{\partial C_j}{\partial t} + U_z \frac{\partial C_j}{\partial z} = D_j \left[\frac{1}{r} \frac{\partial}{\partial r} \left(r \frac{\partial C_j}{\partial r} \right) + \frac{\partial^2 C_j}{\partial z^2} \right] \quad a_d \frac{\partial C_j}{\partial t} + \beta \cdot \nabla C_j = c \nabla^2 C_j$$

$$-D_j \left(\frac{\partial C_j}{\partial r} \right)_{r=r_{hf}} = k_{g,pore} \left(\frac{p_{a,im}^s}{R_s T} \right) \quad -D_j \left(\frac{\partial C_j}{\partial R} \right)_{R=1} = \frac{k_{g,pore}}{r_{hf}} \left(\frac{p_{a,im}^s}{R_s T} \right)$$

$$\left(\frac{\partial C_j}{\partial r} \right)_{r=0} = 0 \quad C_{j,z=0} = C_{tan k} \quad a_d = 1 \quad \beta = \left[\frac{-D_j r_{hf}}{2U} \left(\frac{R^2}{L} \right) \right]$$

$$V \frac{dC_{tan k}}{dt} = Q(C_{j,z=L} - C_{tan k}) \quad p_{a,im}^s = \left(\frac{H_s C_{j,z=L}}{1 + \frac{K_b}{10^{pH-14}}} \right) \quad c = \begin{bmatrix} \frac{D}{r_{hf}^2} & 0 \\ 0 & \frac{D}{L^2} \end{bmatrix}$$

$$C_{j,z=0} = C_{tan k}$$

Figure 5. Equations

Figure 6 shown the domain and how the concentration is decreasing when the fluid pass trough a fiber. At R=1 the transport of the ammonia trough the membrane to the acid solution is occurring.

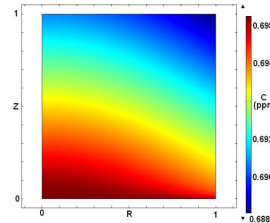


Figure 6. Distribution of Cj over a the domain, inside the fiber at t=10000s.

Results: From the Figure 7-a is evident that this model is independent of the initial concentration set in the tank. According to 7-b and 7-c, the improvement in the efficiency of this separation process by rising the pH or the flow rate is limited. Similar qualitative behavior is present in previous works¹⁻⁴. Some experiments were done to test the performance of the model. Some deviation were observed figure 7-d experiment, but nevertheless, a good agreement were observed between experimental and simulated values.

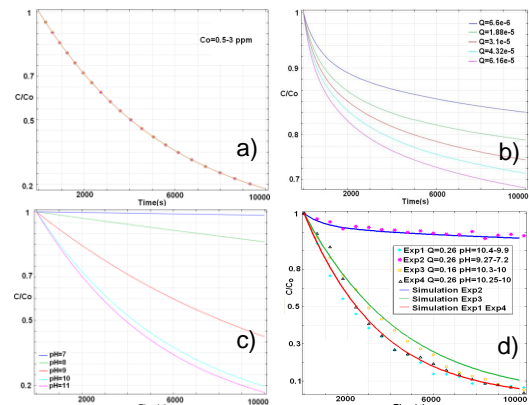


Figure 7. Evolution of concentration in the feeding tank at different conditions.

Conclusions: This model can be used to evaluate the hollow fiber membrane contactors performance for ammonia removal from aqueous solutions under different processing conditions and to define the operational parameters necessary to remove ammonia efficiently. More rigorous approaches will be taken in to account in further works where the model include the solution for the hydrodynamics inside the membrane contactor.

Acknowledgements: This study has been supported by the ZERODISCHARGE project (CPQ2011-26799) financed by Ministry of Science and Innovation and the Catalan government (project ref. 2009SGR905).

References:
 1, Mandowara and Bhattacharya, J. of Envir. Manag., 92, 121-130 (2011)
 2, Mandowara and Bhattacharya, Compu. and Chem. Eng., 33, 1123-1131 (2009)
 3, Aghahari et al., J. of Memb. Sc., 390-391, 164-174 (2012)
 4, Hasanoglu et al., Chem. Eng. J., 160, 530-537 (2010)

12.4 Annex 4. . Paper exhibited in Milan COMSOL Congress in October 2012**Ammonia Removal from Water by Liquid-Liquid Membrane Contactor under Closed Loop Regime.**E. Licon*¹, S. Casas¹, A. Alcaraz¹, J.L. Cortina¹, C. Valderrama¹¹Universitat Politècnica de Catalunya, Barcelona, Spain*Corresponding author: Av. Diagonal 647 Edif. H 4th floor Barcelona, Spain 08028, edxon.eduardo.licon@upc.edu

Abstract: Ammonia separation from water by a membrane contactor was simulated on transient state and compared with experimental data. Aqueous low concentrated solution of ammonium with high pH has been pumped inside a hydrophobic hollow fiber (lumen), sulfuric acid solution in the outside part and the feeding solutions are in closed loop configuration. In order to simulate the separation process, the model equations were developed considering radial-axial diffusion and convection in the lumen with a well-developed parabolic velocity profile. The model proposed shows minimal deviations when is compared against experimental data. This study shows that the most important parameters to control during the operation are the flow rate and the pH, mainly the last one, due to high dependence in chemical equilibrium of ammonium reaction to ammonia.

Keywords: Ammonia removal, Membrane contactor, recirculation.

1. Introduction

In this Study, water of a waste water treatment plant was used to remove ammonium by a liquid-liquid membrane contactor. This technology will be applied in the Hydrogen and Oxygen production by electrolysis via renewable energies, an outline of the process is shown in Appendix. The aim of this work relies on fulfill the process requirements in the electrolysis, since the efficiency of this step is

inversely proportionally to conductivity. The ammonia concentration before membrane distillation step is usually between 1-5 ppm with not variations after this process. Then to use a liquid-liquid membrane contactor is proposed to reduce ammonium (NH_4^+) concentration before Membranes distillation step.

1.1 Ammonia-Ammonium equilibrium

Ammonia is a colorless gas with a characteristic odor, very soluble in water. Its aqueous solutions are alkaline and have a corrosive effect in front to metals and tissue. Ammonia in water exists in

free and ionic forms under equilibrium as is shown in equation 1:

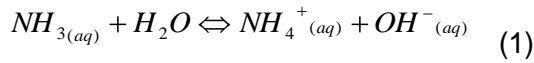


Figure 1 shows the predominant species for the ammonium equilibrium in water at different values of pH. For values below the pK_a (9.3), ion ammonium is greater than ammonia. When pH is higher than the pK_a , we found ammonia as predominant compound. Ammonia reacts with OH-ions present in the water, leading to gaseous ammonia molecule NH_3 . This gas pass through the hydrophobic membrane porous and reacts with an acid solution, where it is immediately dissolved as is shown in Figure 2-b. Since the membrane is hydrophobic, it prevents passage of feed aqueous solution through the pores and the pores are filled with air.

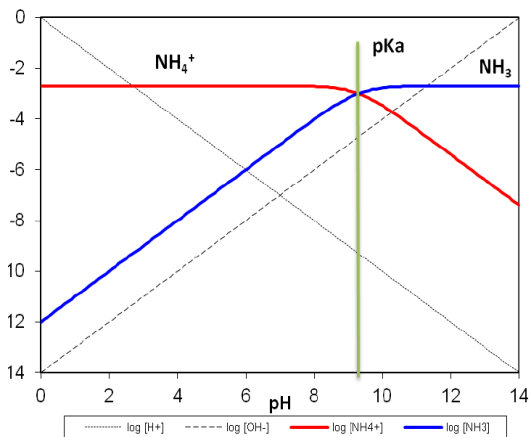


Figure 1. Dependence of the Ammonia-Ammonium equilibrium with respect to pH.

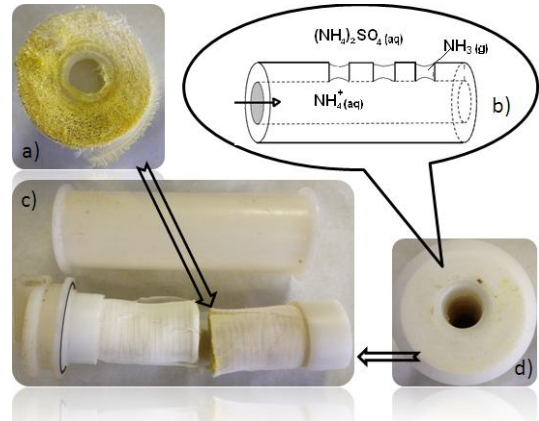


Figure 2. a) Cross section of a membrane module showing the fibers. b) Hollow fiber with the transport phenomena. c) Membrane contactor. d) Side view of the entrance to the hollow fibers.

2. Experimental

2.1 Materials

The hydrophobic membrane contactor HFMC, (Liqui-Cel X30HF, Celgard, USA), consists on hollow fibers, its properties are given in the Appendix (Table 1). The reagents used were ammonium chloride, sodium hydroxide to increase the pH of the dissolution, sulfuric acid (H_2SO_4 98% v/v) in the receiving compartment and borax as a buffer for maintain the pH in the feeding tank.

2.2 Set-up and procedure

Aqueous solutions of NH_3 were prepared by dissolving ammonium chloride in water for concentrations between 5 and 15 ppm, which will be referred as feeding solutions. The pH of the feed solutions was set higher than the usual value of pK_a with

NaOH. Borax buffer has been used to keep the pH. The acid solution was prepared dissolving 5 ml of H_2SO_4 in 5 L of water. The concentration of dissolved NH_3 in the water was measured by Ion Chromatography System (ICS-1000 Dionex, USA). The solution pH was measured by pH meter (pH meter GLP22 Crison, Spain).

Figure 3 shows the experimental set-up used in the present study. It consisted on the HFMC module, two peristaltic pumps and two tanks, one for the ammonium solution and the other for the receiving solution.

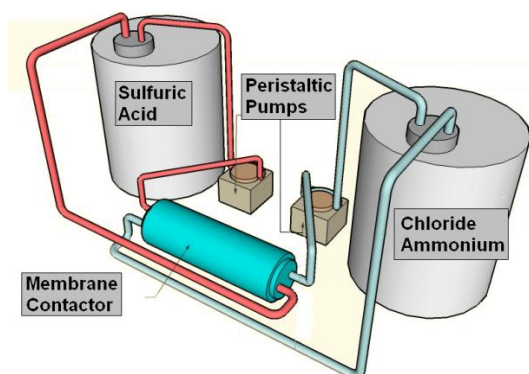


Figure 3. Experimental setup.

The feed was delivered inside the hollow fiber (lumen) with different flow rates from a 10L tank containing aqueous NH_4^+ solution and was continuously recycled. In the other hand, the acid solution contained in a 5 L tank was delivered in the outside of the fibers inside the HFMC (shell) side of the module at constant flow rate in a countercurrent mode and was

continuously recycled. Different conditions of pH, flow rate and initial concentration were tested.

At regular time intervals of 10 min, samples of 20ml were taken from the feed tank by opening. Then each sample was analyzed by chromatography system.

At the end of the experiment, both flows were stopped. The system was properly shut down and cleaned by passing DI water through both sides to remove the remaining solution.

3. Equations

Following assumptions that have been made for some authors¹⁻⁴, it has been considered: unsteady state and isothermal conditions, Henry's law is applicable for feed-membrane interface, no pore blockage occurs, the feed aqueous solution do not fills the membrane pores, the reaction of ammonia with the sulfuric acid is instantaneous and always occurs in excess. Flow rates of both ammonia solution and sulfuric acid are constant and Feed tank operates at the perfect mixing mode.

The transport of both ammonia and ammonium ions in the lumen is expressed through a convective-diffusive equation:

$$\frac{\partial C_j}{\partial t} + \tilde{U} \cdot \nabla C_j = D_j \nabla^2 C_j + R_j \quad (2)$$

where C_j is concentration of ammonia and ammonium ions ($\text{mol}\cdot\text{m}^{-3}$), D is diffusivity of the component in water ($\text{m}^2\cdot\text{s}^{-1}$), R_j is the rate of generation due to the chemical reaction ($\text{mol}\cdot\text{s}^{-1}\cdot\text{m}^{-3}$), U is the velocity vector ($\text{m}\cdot\text{s}^{-1}$).

In this process there is no chemical reaction in the lumen side, so the symmetry assumed inside the lumen is cylindrical. Further, U_r (Radial velocity), which is due to the diffusion of ammonia in the radial direction, also becomes zero. This is because the rate of diffusion of ammonia in water is negligible and the flow is in the Z direction. Now, the equation can be modified as follows:

$$\frac{\partial C_j}{\partial t} + U_z \frac{\partial C_j}{\partial Z} = D_j \left\{ \frac{1}{r} \frac{\partial}{\partial r} \left(r \frac{\partial C_j}{\partial r} \right) + \frac{\partial^2 C_j}{\partial Z^2} \right\} \quad (3)$$

The velocity distribution in the fiber under laminar flow conditions can be written as:

$$U_z(r) = 2\bar{U} \left\{ 1 - \left(\frac{r}{r_{hf}} \right)^2 \right\} \quad (4)$$

r is radial coordinate (m) and r_{hf} is radius of the fiber. Defining \bar{U} to be the average velocity of the fluid inside the lumen:

$$\bar{U} = \frac{Q}{N\pi r_{hf}^2} \quad (5)$$

Q is the flow rate (m^3/s) and N is the number of fibers in the HFMC. Once defined the equations for the mass balance within fiber, the boundary conditions are:

$$C_{j,Z=0} = C_{\text{tank}} \quad (6)$$

$$\left(\frac{\partial C_j}{\partial r} \right)_{r=0} = 0 \quad (7)$$

$$-D_j \left(\frac{\partial C_j}{\partial r} \right)_{r=r_{hf}} = k_{g,pore} \left(\frac{P_{a,int}^g}{R_g T} \right) \quad (8)$$

It can be seen that the flux of ammonia in aqueous phase equals the flux of the gaseous ammonia diffused through the pore as defines equation (8). For determinate the equation (8) must be defined the mass transfer coefficient inside the pore (m/s):

$$k_{g,pore} = D_{a,c,pore} \left\{ \frac{\varepsilon}{\tau b} \right\} \quad (9)$$

$D_{a,c,pore}$ is diffusivity of ammonia ($\text{m}^2\cdot\text{s}^{-1}$), ε is porosity of the membrane, b is membrane thickness (m) and τ is tortuosity of the pore given by:

$$\tau = \frac{1}{\varepsilon^2} \quad (10)$$

Diffusivity of ammonia in the pore is calculated by:

$$\frac{1}{D_{a,c,pore}} = \frac{1}{D_{k,a,pore}} + \frac{1}{D_{a,air}} \quad (11)$$

$D_{k,a,pore}$ is Knudsen diffusion ($m^2 \cdot s^{-1}$), $D_{a,air}$ is diffusivity of ammonia in the air ($m^2 \cdot s^{-1}$). Further, the Knudsen diffusion is given by:

$$D_{k,a,pore} = \frac{d_{pore}}{3} \left(\frac{8R_g T}{\pi M_a} \right)^{1/2} \quad (12)$$

d_{pore} is diameter of pore (m), R_g is universal gas constant ($J \cdot mol^{-1} \cdot K^{-1}$), T is temperature (K) and M_a is molecular weight of ammonia ($g \cdot mol^{-1}$). As previously defined, C_j is the concentration of ammonia and ammonium ions ($mol \cdot m^{-3}$):

$$C_j = [NH_3] + [NH_4^+] \quad (13)$$

Where $[NH_3]$ is concentration of ammonia ($mol \cdot m^{-3}$) and $[NH_4^+]$ is concentration of ammonium. On the other hand, at the liquid-gas interface located at the pore interface, Henry's law may be applicable:

$$P_{a,int}^g = H_a \cdot [NH_3]_{int} \quad (14)$$

H_a is Henry's constant ($Pa \cdot m^3 \cdot mol^{-1}$) and $[NH_3]_{int}$ is concentration of ammonia at

liquid-gas interface ($mol \cdot m^{-3}$). As explained at the previous section 1.1, in aqueous solution equilibrium is established between dissolved ammonia gas and ammonium ions, where according to equation (1) the ionization constant of ammonia is.

$$k_b = \frac{[NH_4^+][OH^-]}{[NH_3]} \quad (15)$$

Since the pH is maintained during the process, the concentration of OH^- is kept constant in the lumen and is given by

$$[OH^-] = 10^{pH-14} \quad (16)$$

Substituting the equation 16 in equation 15 it is observed that k_b is a function of pH. At higher pH values, the k_b will be smaller and the equilibrium move towards the formation of ammonium. By the other hand, a mass balance over ammonia tank under the assumption of uniform mixing can be written:

$$V \frac{dC_{tank}}{dt} = Q(C_{j,z=L} - C_{tank}) \quad (18)$$

Initial Condition: at $t=0$

$$C_0 = C_{tank} \quad (19)$$

4. Use of COMSOL Multiphysics

One single hollow fiber is simulated using a 2D axisymmetric model. The equations were nondimensionalized only in terms of the aspect

ratio of the fiber, then in order to solve equation (3) using the PDE coefficient form the coordinates are $Z=z/L$ and $R=r/r_{hf}$, where L and r_{hf} are the hollow fiber length and radius respectively. The coefficient values for the settings of the coefficient form would be:

Diffusion coefficient:

$$c = \begin{bmatrix} \frac{D}{r_{hf}^2} & 0 \\ 0 & \frac{D}{L^2} \end{bmatrix} \quad (20)$$

Convection coefficient

$$\beta = \begin{bmatrix} -D/r_{hf} \\ 2\bar{U}(-R^2)/L \end{bmatrix} \quad (21)$$

Mass coefficient

$$d_a = 1 \quad (22)$$

In order to obtain the transport phenomena in the boundary condition equal to $R=1$, a flux boundary condition is set:

$$-D_j \left(\frac{\partial C_j}{\partial R} \right)_{R=1} = \frac{k_{g,pore}}{r_{hf}} \left(\frac{p_{a,int}^g}{R_g T} \right) \quad (23)$$

The partial pressure of ammonia in the interface is according to equations 9-16:

$$p_{a,int}^g = \frac{H_a C_{j,R=1}}{\left(1 + \frac{K_b}{10^{pH-14}} \right)} \quad (24)$$

Recirculation is taken into account as a boundary condition in $Z=1$, where equation (18) is taken in to account as a global equation that describes the concentration in the tank:

$$C_{j,Z=0} = C_{\tan k} \quad (25)$$

The pH of the solution in the tank was considered as a time dependant function, fitted in a previous step in MATLAB from experimental results with the equation (26), see Figure 3.

$$pH(t) = pH_0 + \frac{pH_{end} - pH_0}{6.58 \cdot 10^4 + t^{3/2}} \quad (26)$$

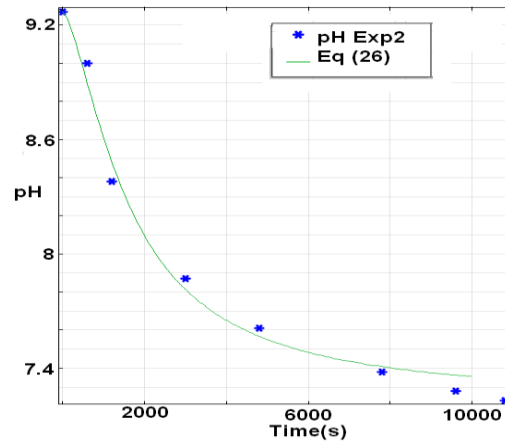


Figure 4. Evolution of pH in an experiment without buffer solution.

5. Results:

In the Figure 5 is shown how the concentration is decreasing when the fluid pass the lumen of a fiber, at $R=1$ the transport of the ammonia trough the membrane to the acid solution is occurring. Different simulations have been done.

From the Figure 6 is evident that this model is independent of the initial concentration set in the tank with ammonium chloride. According to Figure 7 and Figure 8, the improvement in the efficiency of this separation process by rising the pH or the flow rate is limited by some extend and this information can be used to optimize resources and energy needed to carry out the operation. This information is in agreement with the results obtained in

previous works done before without the use of COMSOL^{1,2}

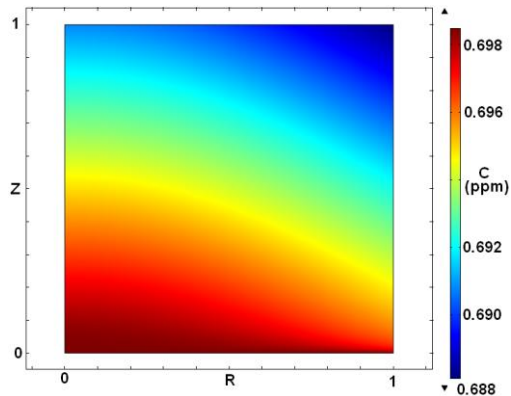


Figure 5. Distribution of C_j over plane inside the fiber for a $t=10000$ seconds.

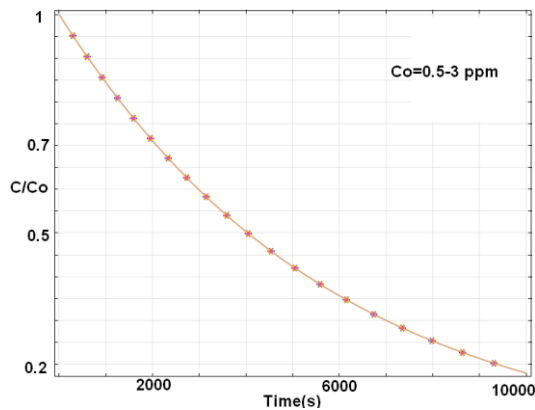


Figure 6. Normalized concentration evolution in the feeding tank at different initial concentrations from 0.5 ppm of ammonium to 3 with a $Q=4.392e-6$ m³/s and pH=10.3.

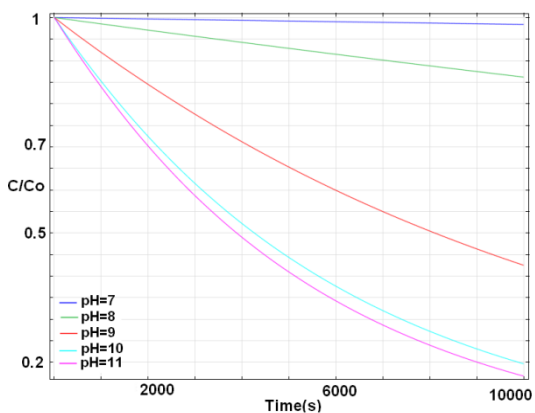


Figure 7. Normalized concentration evolution in the feeding tank at different pH at $Q= 4.392e-6$ m³/s and $Co=15$ ppm.

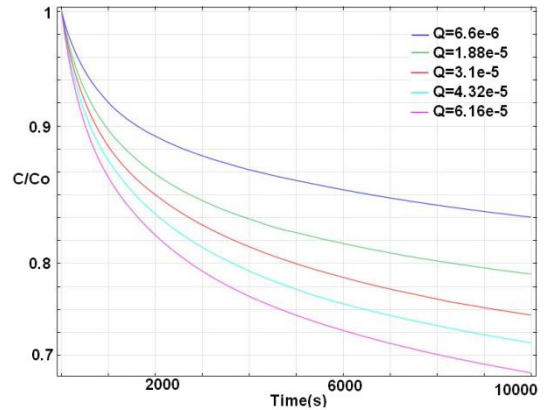


Figure 8. Normalized concentration evolution in the feeding tank at different flow rates (Q in m³/s) $Co=15$ ppm and pH=10.3.

Some experiments were done to test the performance of the model. In Figure 6 is shown the evolution of the tank concentration under different experimental conditions in terms of flow rate and initial pH, as well as the predicted values. In the experiment 2 a poor removal of NH^{+4} was obtained because no buffer solution was added and pH was not constant. Next experiments were made with initial buffered solution. The experiment 1 and 4 were performed under same conditions but the solutions were prepared on tap water and distillate water, respectively. Some deviation were observed in tap water experiment, but nevertheless, a good agreement were observed between experimental and simulated values.

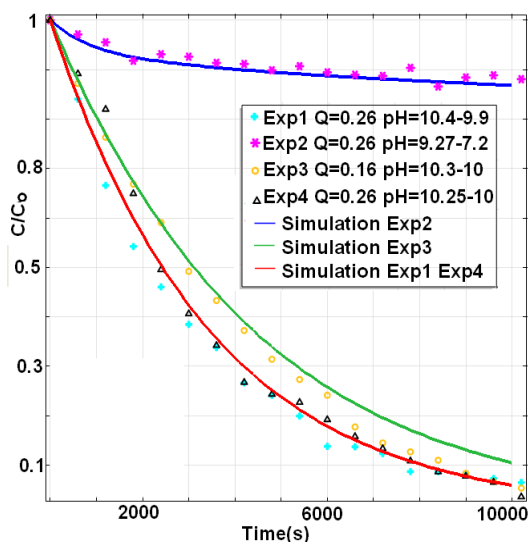


Figure 9. Comparison of the evolution in different experiments of the concentration in the feeding tank with its respective simulation.

6. Conclusions

The use a liquid-liquid membrane contactor to improve the water quality used in the production of hydrogen is a good option. When the process is carry out in closed loop there are no emotions to the atmosphere and this contributes to make the process safe and environmentally friendly.

This model can be used to evaluate the hollow fiber membrane contactors performance for ammonia removal from aqueous solutions under different processing conditions and to define the operational parameters necessary to remove ammonia efficiently.

The membrane contactor model proposed is suitable for prediction of ammonium removal in view the minimal deviations when compared to the experimental data. The most important parameters to control during the experiment are the flow rate and the pH, mainly the last one, due to the high dependence in the chemical equilibrium of ammonium reaction to ammonia.

Finally, the use of COMSOL makes easier and faster to solve the equations proposed in the model for liquid-liquid contactor.

More rigorous approaches will be taken in to account in further works where the model include the solution for the hydrodynamics inside the membrane contactor and open loop regime will be evaluated.

7. References

1. Mandowara and Bhattacharya, Simulation studies of ammonia removal from water in a membrane contactor under liquid-liquid extraction mode, *Journal of Environmental Management*, **92**, 121-130 (2011)
2. Mandowara and Bhattacharya, Membrane contactor as degasser operated under vacuum for ammonia removal from water: A numerical simulation of mass transfer under laminar flow conditions, *Computers and Chemical Engineering*, **33**, 1123–1131 (2009)
3. Agrahari et al., Model prediction and experimental studies on the removal of dissolved NH₃ from water applying hollow fiber membrane contactor, *Journal of Membrane Science*, **390–391**, 164–174 (2012)
4. Hasanoglu et al., Ammonia removal from wastewater streams through membrane contactors: Experimental and theoretical analysis of operation parameters and configuration, *Chemical Engineering Journal*, **160**, 530–537 (2010)

8. Acknowledgements

This study has been supported by the ZERODISCHARGE project (CPQ2011-26799) financed by Ministry of Science and Innovation

and the Catalan government (project ref. 2009SGR905).

9. Appendix

Table 1: Properties of the membrane contactor.

Membrane Contactor Property	Typical Values	Units
Porosity	40	%
Pore Dimensions	0.04 x 0.10 μm	μm
Effective Pore Size	0.04	μm
Burst Strength	220	PSI (15.5 kg/cm ²)
Tensile Break Strength	175	gr/filament
Resistance to Air Flow	25-45	Gurley sec.
Shrinkage, Axial Direction	5	%
Internal Diameter	240	μm
Wall Thickness	30	μm
Outer Diameter	300	μm

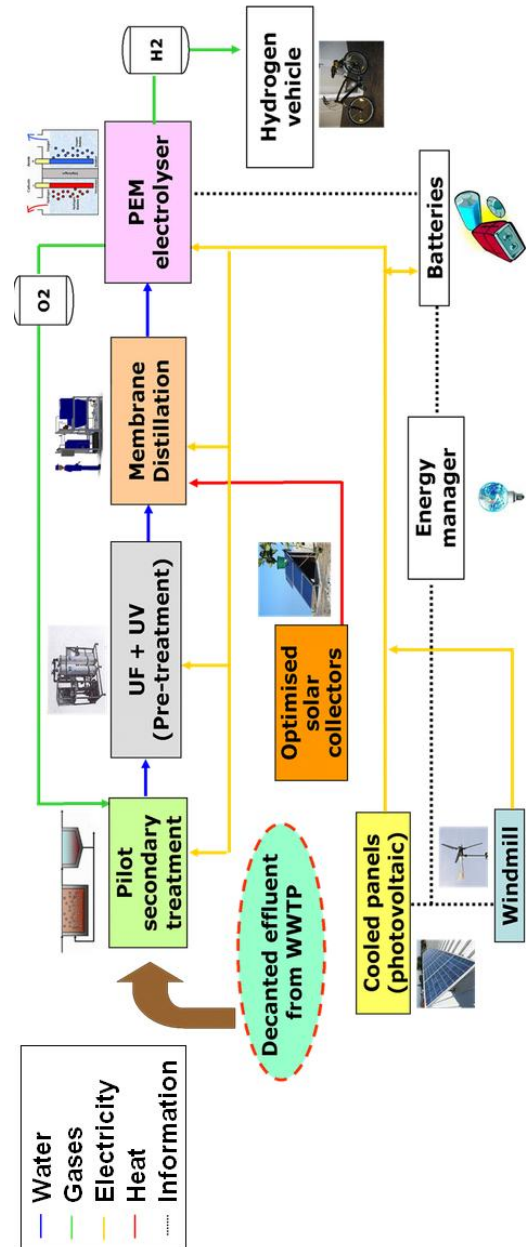


Figure 10. Outline of the Greenlysis project.

13. References

Agrahari G., Shukla S., Verma N., Bhattacharya P., 2012. Model prediction and experimental studies on the removal of dissolved NH₃ from water applying hollow fiber membrane contactor. *Journal of Membrane Science* 390–391, 164–174.

Albrecht W., Hilke R., Kneifel K., Weigel Th., Peinemann K.V., 2005. Selection of microporous hydrophobic membranes for use in gas/liquid contactors: an experimental approach. *Journal of Membrane Science* 263, 66-76

Al-Marzouqi M., El-Naas M., Marzouk S., Abdullatif N., 2008. Modeling of chemical absorption of CO₂ in membrane contactors. *Separation and Purification Technology* 62, 499–506

Ashrafizadeh S.N., Khorasani Z., 2010. Ammonia removal from aqueous solutions using hollow-fiber membrane contactors *Chemical Engineering Journal*. 162, 242-249

Atcharyawut S., Fena C., Jiratananon R., Liang D.T., 2006. Effect of membrane structure on mass-transfer in the membrane gas-liquid contacting process using microporous PVDF hollow fibers. *Journal of Membrane Science* 285, 272-281

Baker R. W., 2000. *Membrane technology and applications*. McGraw-Hill. 189-210

Baset D.C., 1985. Poly (vinylidene fluoride), development in crystalline polymers. *Applied Science*, vol. 1

Bottino A., Capannelli G., Comite A., Di Felice R., Firpo R., 2008. CO₂ removal from a gas stream by membrane contactor. *Separation and Purification Technology* 59, 85-90

Bottino A., Capannelli G., Comite A., Firpo R., Felice R.D., Pinacci P., 2006. Separation of carbon dioxide from flue gases using membrane contactors, *Desalination* 200, 609–611.

Busca G. and Pistarino C., 2003. Abatement of ammonia and amines from waste gases: a summary. *Journal of Loss Prevention in the Process Industries* 16, 157–163.

Dindore V.Y., Brillman D.W.F., Feron P.H.M., Versteeg G.F., 2004. CO₂ absorption at elevated pressures using a hollow fiber membrane contactor, *Journal of Membrane Science* 235, 99–109.

Dindore V.Y., Versteeg G.F., 2005. Gas–liquid mass transfer in a cross-flow hollow fiber module: analytical model and experimental validation, *International Journal of Heat and Mass Transfer* 48, 3352–3362.

Feron, P.H.M., Jansen, A.E. and Klaassen, R., 1997, Membrane gas absorption: a new membrane technology for gas separation and purification, 6th Aachener Membran Kolloquium, 3–5

Gabelmana A., Hwangb S., 1999. Hollow fiber membrane contactors. *Journal of Membrane Science* 159, 61-106

Ghogomu J.N., Guigui C., Rouch J.C., Clifton M.J., Aptel P., 2001. Hollow-fiber membrane module design: comparison of different curved geometries with Dean vortices, *Journal of Membrane Science* 181, 71–80.

Ho, W.S.W. and Poddar, T.K., 2001. New membrane technology for removal and recovery of chromium from waste waters, *Environmental Progress*, 20(1): 44–52.

Jorgense TC, Wheatley LR, 2003. Ammonia removal from wastewater by ion exchange in the presence of organics contaminants, *Water Research*. 37, 1723-1728

Keshavarz P., Ayatollahi S., Fathikalajahi J., 2008. Mathematical modeling of gas-liquid membrane contactors using random distribution of fibers. *Journal of Membrane Science* 325, 98–108

Kiani A., Prasad R., Bhave R.R., Sirkar K.K., 1984. Solvent extraction with immobilized interfaces in a microporous hydrophobic membrane, *Journal of Membrane Science* 20, 125–145

Kim Y.S., Yang S.M., 2000, Absorption of carbon dioxide through hollow fiber membranes using various aqueous absorbents, *Separation and Purification Technology* 21, 101–109

Klaassen R., Feron P., Jansen A., 2008. Membrane contactor applications. *Desalination* 224, 81–87

Klaassen R., Jansen A.E., Bult B.A., Oesterholt F., Schneider J., 1994b. Removal of hydrocarbons from waste water by pertraction, *Proc. 7th International Symposium on Synthetic Membranes in Science and Industry, Tübingen, Germany*, 316–319.

Klaassen, R. and Jansen A.E., 2001, The membrane contactor: environmental applications and possibilities, *Environmental Progress* 20(1) 37–43.

Klaassen, R., Feron, P. H. M. and Jansen, A. E., 1996. Membrane gas absorption environmental applications, *Proceedings ICOM. 96*, 916–917.

Klaassen, R., 1998. Vom Abwasser zum Wertstoff, *Chemie Umwelt Technik* 24–28.

Klassen R., Feron P., Jansen A., 2005. Membrane contactors in industrial applications. *Chemical Engineering Research and Design* 83, 234–246

Kreulen H., Smolders C., Versteeg G.F., Van Swaaij W.P.M., 1993. Microporous hollow fiber membrane modules as gas-liquid contactors. Part 1. Physical mass transfer processes: a specific application: Mass transfer in highly viscous liquids, *Journal of Membrane Science* 78, 197–216.

Lee K., Yeon S., Sea B., Park Y., 2004. Hollow Fiber Membrane Contactor Hybrid System for CO₂ Recovery. *Studies in Surface Science and Catalysis* 153, 423-428

Lee Y., Noble R., Yeom B., Park Y., Lee K., 2001. Analysis of CO₂ removal by hollow fiber membrane contactors. *Journal of Membrane Science* 194, 57–67

Lee Y., Noble R.D., Yeon B.Y., Park Y.I., Lee K.H., 2001. Analysis of CO₂ removal by hollow fiber membrane contactors, *Journal of Membrane Science* 194, 57–67

Licon E., Casas S., Alcaraz A., Cortina J.L., Valderrama C., 2012, Ammonia Removal from Water by Liquid-Liquid Membrane Contactor under Closed Loop Regime, *Proceedings of the European Comsol Conference held in Milan October 2012*

Liu L., Li L., Ding Z., Ma R., Yang Z., 2005. Mass transfer enhancement in coiled hollow fiber membrane modules, *Journal of Membrane Science* 264, 113–121.

Mallubhotla H., Schmidt M., Lee K.H., Belfort G., 1999. Flux enhancement during Dean vortex tubular membrane nanofiltration: 13. effects of concentration and solute type, *Journal of Membrane Science* 153, 259–269.

Mandowara A., Bhattacharya P, 2009. Membrane contactor as degasser operated under vacuum for ammonia removal from water: A numerical simulation of mass transfer under laminar flow conditions. *Computers and Chemical Engineering* 33, 1123–1131

Mandowara A., Bhattacharya P., 2011. *Journal of Environmental Management* 92, 121-130.

Manno P., Moulin P., Rouch J.C., et al., 1998. Mass transfer improvement in the helicallywound hollowfiber ultrafiltration modules Yeast suspensions, *Separation and Purification Techno*14, 175–182.

Mansourizadeh A., Ismael A.F., 2009. Hollow fiber gas-liquid membrana contactors for acid gas capture: A review. *Journal of Hazardous Materials* 171, 38-53

McDermott C., Tarafder S., Kolditz O., Schüth C., 2007. *Journal of Membrane Science* 292, 17–28

Moazed H., 2008. Ammonium ion removal from wastewater by a natural resin. *Journal Environmental Science Technology*. 1, 11-18

Rezakazemi M., Shirazian S., Ashrafizadeh S., 2012. Simulation of ammonia removal from industrial wastewater streams by means of a hollow-fiber membrane contactor. *Desalination*. 285, 383-392

Sarioglu, M. 2005. Removal of ammonium from municipal wastewater using natural Turkish (Dogantepe) zeolite. *Separation and purification Technology* 41, 1-11.

Scott K., 1998. Section 4 - Air and gas filtration and cleaning. *Handbook of Industrial Membranes (Second Edition)*, 309-327.

Tan X., Tan S.P., Teo W.K., Li K., 2006. Polyvinylidene fluoride (PVDF) hollow fibre membranes for ammonia removal from water. *Journal of Membrane Science* 271, 59-68.

Tan X., Tan S.P., Teo W.K., Lia L., 2006. Polyvinylidene fluoride (PVDF) hollow fibre membranes for ammonia removal from water, *Journal of Membrane Science* 271, 59–68.

Wehner J.F., Wilhelm R.H., 1956. Boundary conditions of flow reactor. *Chemical Engineering Science* 6, 89-93

Wickramasinghe S.R., Semmens M.J., Cussler E.L., 1998. Mass transfer in various hollow fiber geometries, *Journal of Membrane Science* 69, 235–250.

Yang M.C., Cussler E.L., 1986. Designing hollow-fiber contactors, *AIChE Journal* 32, 1910–1916.

Zhang Q., Cussler E.L., 1985. Microporous hollow fibres for gas absorption I. Mass transfer in the liquid, *Journal of Membrane Science* 23, 321–332.

Zhu Z., Hao Z., Shen Z., Chen J., 2005. Modified modeling of the effect of pH and viscosity on the mass transfer in hydrophobic hollow fiber membrane contactors, *Journal of Membrane Science* 250, 269-276

Zhu Z., Hao Z., Shen Z., Chen J., 2005. Modified modeling of the effect of pH and viscosity on the mass transfer in hydrophobic hollow fiber membrane contactors, *Journal of Membrane Science* 250, 269–276.

